PLOS ONE

RESEARCH ARTICLE

Biogeochemical dynamics and microbial community development under sulfate- and iron-reducing conditions based on electron shuttle amendment

Theodore M. Flynn[1¤], Dionysios A. Antonopoulos[1], Kelly A. Skinner[1], Jennifer M. Brulc[1], Eric Johnston[1], Maxim I. Boyanov[1,2], Man Jae Kwon[1,3], Kenneth M. Kemner[1], Edward J. O'Loughlin[1]*

1 Biosciences Division, Argonne National Laboratory, Lemont, Illinois, United States of America, **2** Institute of Chemical Engineering, Bulgarian Academy of Sciences, Sofia, Bulgaria, **3** Department of Earth and Environmental Sciences, Korea University, Seoul, South Korea

¤ Current address: California Department of Water Resources, West Sacramento, California, United States of America
* oloughlin@anl.gov

Citation: Flynn TM, Antonopoulos DA, Skinner KA, Brulc JM, Johnston E, Boyanov MI, et al. (2021) Biogeochemical dynamics and microbial community development under sulfate- and iron-reducing conditions based on electron shuttle amendment. PLoS ONE 16(5): e0251883. https://doi.org/10.1371/journal.pone.0251883

Editor: John M. Senko, The University of Akron, UNITED STATES

Received: December 18, 2020

Accepted: May 4, 2021

Published: May 20, 2021

Data Availability Statement: Raw sequence data are publicly available through MG-RAST under project number mgp96975. https://www.mg-rast.org/mgmain.html?mgpage=project&project=mgp96975.

Funding: This research and all authors were supported by the US Department of Energy, Office of Biological and Environmental Research (https://www.energy.gov/science/ber/biological-and-environmental-research), as part of Subsurface

Abstract

Iron reduction and sulfate reduction are two of the major biogeochemical processes that occur in anoxic sediments. Microbes that catalyze these reactions are therefore some of the most abundant organisms in the subsurface, and some of the most important. Due to the variety of mechanisms that microbes employ to derive energy from these reactions, including the use of soluble electron shuttles, the dynamics between iron- and sulfate-reducing populations under changing biogeochemical conditions still elude complete characterization. Here, we amended experimental bioreactors comprised of freshwater aquifer sediment with ferric iron, sulfate, acetate, and the model electron shuttle AQDS (9,10-anthraquinone-2,6-disulfonate) and monitored both the changing redox conditions as well as changes in the microbial community over time. The addition of the electron shuttle AQDS did increase the initial rate of Fe^{III} reduction; however, it had little effect on the composition of the microbial community. Our results show that in both AQDS- and AQDS+ systems there was an initial dominance of organisms classified as *Geobacter* (a genus of dissimilatory Fe^{III}-reducing bacteria), after which sequences classified as *Desulfosporosinus* (a genus of dissimilatory sulfate-reducing bacteria) came to dominate both experimental systems. Furthermore, most of the ferric iron reduction occurred under this later, ostensibly "sulfate-reducing" phase of the experiment. This calls into question the usefulness of classifying subsurface sediments by the dominant microbial process alone because of their interrelated biogeochemical consequences. To better inform models of microbially-catalyzed subsurface processes, such interactions must be more thoroughly understood under a broad range of conditions.

Biogeochemical Research Program's (https://www.doesbr.org) Scientific Focus Area (SFA) at Argonne National Laboratory (Argonne). Argonne is a U.S. Department of Energy laboratory managed by UChicago Argonne, LLC. under contract DE-AC02-06CH11357. MRCAT/EnviroCAT operations are supported by DOE and the MRCAT/EnviroCAT member institutions. Use of the Advanced Photon Source, an Office of Science User Facility operated for the U.S. Department of Energy (DOE) Office of Science by Argonne, was supported by the U.S. DOE under Contract No. DE-AC02- 06CH11357. The funders had no role in study design, data collection and analysis, decision to publish, or preparation of the manuscript.

Competing interests: The authors have declared that no competing interests exist.

Introduction

The biogeochemical cycling of carbon (C), iron (Fe), and sulfur (S) in aquatic and terrestrial environments is driven largely by microbially-catalyzed redox reactions. Such reactions by definition involve the transfer of electrons, so it is necessary to assess the thermodynamic and kinetic constraints on electron transfer in appropriate model systems in order to understand the metabolic processes that drive these biogeochemical cycles. For example, in many environments ferric iron (Fe^{III}) is primarily present as relatively insoluble Fe^{III} oxides. These minerals provide an important electron sink during anaerobic respiration by a variety of dissimilatory Fe^{III}-reducing bacteria (DIRB) and archaea. These phylogenetically diverse microorganisms are able to obtain energy by coupling the oxidation of organic compounds or molecular hydrogen to the reduction of Fe^{III} to Fe^{II} under suboxic and anoxic conditions [1–3]. Fe^{III}-reducing microorganisms and the reactive ferrous species they produce play a major role in controlling water quality [4,5], the dissolution and precipitation of minerals [6–8], nutrient availability [9], and the fate and transport of contaminants [10].

Due to the relative insolubility of ferric minerals in most environments, DIRB must employ different mechanisms to respire using these terminal electron acceptors than those used for soluble terminal electron acceptors such as dissolved oxygen (O_2), nitrate (NO_3^-), and sulfate (SO_4^{2-}) [11]. Some DIRB such as *Geobacter* and *Shewanella* can transfer electrons directly to Fe^{III} oxide surfaces by means of reductases located on their outer cell membrane [12] or via electrically conductive pili or nanowires [13–17]. The need for physical contact between Fe^{III} oxide minerals and microbial cells, however, can be readily overcome. The dissolution of Fe^{III} oxides is promoted by exogenous and endogenous ligands and the resulting soluble Fe^{III} complexes can diffuse away and be reduced by DIRB at a distance [18,19]. Likewise, the transfer of electrons from the cell to external electron acceptors (e.g., Fe^{III} oxides) can be facilitated by soluble electron shuttles, i.e., compounds that can be reversibly oxidized and reduced. In this scenario, an oxidized electron shuttle is reduced by the organism, which can transfer electrons to a remote acceptor. Since electron shuttles can be oxidized and reduced repeatedly, they can have a substantial effect on both the rate and extent of Fe^{III} oxide reduction even when present at trace concentrations [20].

A wide variety of endogenous and exogenous organic and inorganic compounds have been shown to function as electron shuttles in the bioreduction of Fe^{III} oxides, including quinones, flavins, phenazines, and reduced sulfur species [20–31]. In addition, humic substances—a class of naturally occurring, chemically heterogeneous organic oligoelectrolytes derived primarily from the decomposition of bacteria, algae, and higher plant material that are ubiquitous in aquatic and terrestrial environments—can also be utilized as electron shuttles in the bioreduction of Fe^{III} oxides [18,30,32–35]. The ability of humic substances to act as electron shuttles has largely been attributed to the presence of quinone groups within their structures [36–38]. However, given the polymorphic nature of humic substances, their structure and functional characteristics are highly variable, including the type and number of reversibly redox active moieties, resulting in a distribution of redox potentials and inherent variability in the redox properties observed among them [38–42]. Therefore, model quinones with well-defined redox characteristics (e.g., reduction potentials) such as 9,10-anthraquinone-2,6-disulfonate (AQDS) have been widely used as analogs for the redox active moieties in humic substances [6,32,43].

A phylogenetically diverse range of bacteria and archaea can transfer electrons to model quinones (e.g., AQDS) and humic substances [44,45]. Indeed, many microorganisms that are not able to reduce Fe^{III} oxides directly, can cause the reduction of Fe^{III} oxides in the presence of a suitable electron shuttle, including organisms that are not primarily categorized as Fe^{III}-reducing microbes (i.e., fermenters, sulfate reducers, and methanogens) [26,27,44,46–49]. The

ubiquity of humic/quinone-reducing microorganisms in aquatic and terrestrial environments [50] and the ability of reduced humics/quinone to shuttle electrons to Fe^{III} oxides suggests that the presence of electron shuttles provides the potential for bacteria that are not metabolically capable of reducing Fe^{III} minerals to contribute to Fe^{III} oxide bioreduction, thereby increasing microbial diversity under iron-reducing conditions. Although electron shuttles have been shown to significantly enhance Fe^{III} oxide reduction in systems with complex, multispecies microbial communities [51–55], the effects of electron shuttles on microbial community development have not been explicitly examined. In this study, we investigate the effects of the presence and absence of a soluble electron shuttle (AQDS) on biogeochemical dynamics and microbial community development under Fe^{III}- and sulfate-reducing conditions.

Materials and methods

Experimental setup

Experimental bioreactors were created in triplicate using 500 mL serum bottles containing 400 mL of sterile defined mineral medium (pH 7.5). This medium was comprised of HEPES buffer (20 mM), PIPES buffer (20 mM), sodium acetate (10 mM), Na_2SO_4 (5 mM), $CaCl_2$ (5 mM), $MgCl_2$ (1 mM), KCl (0.5 mM), NH_4Cl (1 mM), Na_2HPO_4 (10 μM), $NaHCO_3$ (30 mM), and 10 mL L^{-1} of trace minerals solution [20]. Fe^{III} was provided as natural sienna (Earth Pigments Co.), an iron-rich earth mined from ochre deposits in the Provence region of France that consists primarily of quartz and goethite (α-FeOOH), as determined by powder x-ray diffraction (pXRD) and Fe K-edge extended x-ray absorption fine-structure (EXAFS) spectroscopy. Details of the characterization of natural sienna are provided in Supporting Information (S1 File). Natural sienna was added to the medium at a concentration of 7.6 g L^{-1}; which is equivalent to a total of 30 mmol Fe^{III} per liter of medium. Sieved (400 mesh) quartz (SiO_2) was also added at a concentration of 72 g L^{-1} (Alfa Aesar). In electron shuttle-amended bioreactors, AQDS was added to a final concentration of 100 μM from a sterile, anaerobic stock solution.

Serum bottles were sparged with sterile, O_2-free argon gas and inoculated with 10 grams of sediment obtained from a depth of 7 meters below land surface in a shallow, unconfined alluvial aquifer at the Integrated Field Research Challenge (IFRC) site located at the Old Rifle site (39˚31'44.864"N 107˚46'20.154"W), which is located approximately 0.3 miles east of the city of Rifle in western Colorado [56]. The IFRC is owned by the City of Rifle and The US Department of Energy Office of Legacy Management and its associated researchers were provided access to the site by the City of Rifle through a letter of agreement" [56]. Sediment was taken from sampling well LR-MLS-21 [57] and transported to the lab under anoxic conditions, where it was kept refrigerated at 4 ˚C until added to the bioreactors. Once inoculated, the bioreactors were sealed with plug septa and aluminum crimp caps. The bottles were secured in flask clamps mounted on a roller drum (Bellco Glass, Inc.) and rotated vertically as the long axis of the bottle remained in a horizontal orientation and were incubated in the dark at 25 ˚C. Sterilized (autoclaved, 1 cycle) control bottles were used to test for reduction in the absence of microbial activity.

Experimental systems were subsampled periodically using sterile syringes to measure the production of Fe^{II}, the consumption of acetate and sulfate, and changes in pH. Additional samples were taken at the same time to measure total protein as well as to extract DNA for 16S rRNA gene amplicon sequencing. Unless otherwise indicated, sample collection and processing were conducted in an anoxic glove box (Coy Laboratory Products) containing an anoxic atmosphere (N_2:H_2 = 95:5, O_2 < 1 ppm) and treated as described below for specific geochemical and microbiological assays. Subsamples for microbial community analysis were frozen at −80 ˚C and stored at this temperature until DNA was extracted.

Geochemical analyses

The reduction of Fe^{III} in the bioreactors was monitored by measuring the production of Fe^{II} over time. Samples for total Fe^{II} (i.e., dissolved Fe^{II} and acid-extractable Fe^{II}) analysis were prepared by adding 0.75 mL of anoxic 1 M HCl to a 0.25 mL subsample of the well-mixed bioreactor suspension. The samples were mixed on an end-over-end shaker for two weeks, and then centrifuged at 25,000 × *g* for 10 min. The concentration of Fe^{II} in the supernatant was determined spectrophotometrically using the ferrozine assay [58]. Briefly, 1 mL of HEPES-buffered ferrozine reagent [59] was added to 50 μL of supernatant and the absorbance was measured at 562 nm using a Cary 100 UV-Vis spectrophotometer. The detection limit for ferrous iron using this method is approximately 10 μM.

Samples for sulfate and acetate analysis were prepared by centrifuging a subsample of the well-mixed suspension at 25,000 × *g* for 10 min, then removing 50 μL of supernatant and combining it with 950 μL of an isopropanol solution (15% v:v) to preserve the sample until analysis. The concentrations of sulfate and acetate were measured using a Dionex ICS 3000 ion chromatograph equipped with an IonPac AS11 analytical column (250 × 2 mm, Dionex) and a 1-20 mM KOH eluent gradient at a flow rate of 0.5 mL min^{-1}. The detection limit for these anions was approximately 1 μM.

X-ray absorption spectroscopy

Fe K-edge (7,112 eV) x-ray absorption spectroscopy measurements were carried out at the MR-CAT/EnviroCAT bending magnet beamline (Sector 10, Advanced Photon Source) [60]. The reactor solids were separated by filtration through a 0.22 μm PTFE filter inside the anoxic glove box and the hydrated filter cake was sealed together with the filter between two layers of Kapton film; the filtrate was saved for measurement of dissolved FeII using the ferrozine assay. X-ray absorption near-edge spectra (XANES) and extended x-ray absorption fine structure (EXAFS) spectra were collected at room temperature from the standards and the reactor solids inside a N_2-purged sample cell [61,62]. Anoxic integrity of samples prepared and measured this way have been demonstrated in previous work [63]. Energy calibration was established by setting the inflection point in the spectrum from an Fe foil to 7,112 eV and maintained continuously afterwards by collecting data from the foil simultaneously with the collection of data from the samples. Radiation-induced changes in the spectra were not observed. No differences were observed between spectra from different areas on the sample so all scans from each sample were averaged to produce the final spectrum. Analysis of the spectra involved comparisons to standards followed by linear combination (LC) fitting to extract the spectral weight of up to three standards that best describe the experimental spectra of the bioreactors. More details on the standards and analysis are included in the Supporting Information (S1 File).

DNA extraction, amplification, and sequencing

The samples for microbial community analysis were kept frozen at −80 ˚C until use, when they were thawed for 10 min in a 70 ˚C water bath, then centrifuged at 3,716 × *g* for 10 min. The supernatant was removed, and DNA was extracted from the remaining sediment (~1 g) using the Power Soil DNA Isolation Kit (QIAGEN). Bacterial DNA amount for each sample was then normalized for the overall biomass value at each sample time point. Multiple displacement amplification was performed utilizing phi29 with the GenomiPhi V2 DNA Amplification Kit (GE Healthcare). Protein amounts were also determined for each sample using the bicinchoninic acid-copper (BCA) assay [64] to be used as a marker of biomass value.

Amplicon libraries spanning the V3-V4 region of the 16S rRNA encoding gene (338–802) were constructed using primers to target members of the domain *Bacteria*. The primers

spanned *Escherichia coli* positions 338–802 using 338F (5'-ACTCCTACGGGAGGCAGC-3') and equimolar amounts of the 802R reverse primers (802R-A 5'-TACCRGGGTHTCTAATCC-3', 802R-B 5'-TACCAGAGTATCTAATTC-3', 802R-C 5'-CTACDSRGGTMTCTAATC-3', 802R-D 5'-TACNVGGGTATCTAATCC-3') from the Ribosomal Database Project's (RDP's) Pipeline [65]. Permuted primers containing 10-bp sequences between the sequence adapter (454 Life Sciences A) and the 16S rRNA primer sequence on the forward primer were used to sequence multiple libraries within the same run. PCR reactions were carried out in triplicate for each sample using Platinum® *Taq* High Fidelity polymerase (Invitrogen, ThermoFisher). PCR conditions used an initial denaturation step of 95 ˚C for 3 min, followed by 30 cycles of 95 ˚C for 30 s, 57 ˚C for 45 s, then 72 ˚C for 1 min and finalized by a single extension step 72 ˚C for 2 min. Pooled triplicate product for each sample was then purified using the QIAGEN MinElute® PCR Purification Kit. Amplicon presence, sizing, and concentration was assessed using the Agilent Bioanalyzer DNA 1000 BioChip and equimolar sample pools were prepared for sequencing. 16S rRNA gene amplicons were then sequenced using the 454 Life Sciences Genome Sequencer FLX System and following the manufacturer's protocols. All sequencing and data generation was performed by 454 Life Sciences (Roche) utilizing the XLR70 (Titanium) sequencing chemistry.

Sequencing of 16S rRNA gene amplicons produced a total of 243,565 sequences across 38 samples. Following sequencing, amplicon libraries were processed using a combination of QIIME [66], Acacia [67], and UPARSE [68]. Sequences were demultiplexed and quality filtered using QIIME version 1.9.1. Sequences of poor quality were discarded based on divergence from expected amplicon length (470 bp), quality scores (minimum score 25), long homopolymer runs (max = 6), and primer mismatches (max = 0). All sequences not meeting quality standards (26,305, or 10.7% of the original total) were discarded. Remaining libraries maintained an average sequencing depth of 5,717 ± 2,304 reads.

Remaining sequences were denoised using Acacia then screened for chimeric sequences, dereplicated, and clustered into operational taxonomic units (OTUs) at a 97% similarity cutoff in UPARSE using the -cluster_otus command and the UPARSE-OTU algorithm. Taxonomic identities were assigned to representative sequences from each OTU using the SILVA reference database (version 128) [69]. Singleton OTUs (those containing only a single sequence across all samples) were discarded prior to downstream analyses. Alpha and beta diversity analyses were conducted in the R programming environment using the packages phyloseq [70] and edgeR [71] as well as Primer-7 [72]. Raw sequence data are publicly available through MG-RAST [73] under project number mgp96975.

Results

Geochemical changes in sediment bioreactors

Bioreactors amended with AQDS were compared to unamended controls, monitoring the levels of acetate, Fe^{II}, and sulfate over time. The overall trajectory of these changes can be seen in Fig 1, which can be separated into three distinct phases: an "early" phase occurring over the first 25 days of incubation, a "late" phase lasting from day 25 until sulfate was entirely consumed around day 50, and a "stationary" phase where only minor changes were observed in the chemical composition of the bioreactors. Visually, the initial light tan color of the reactors changed over the course of the experiment to a dark gray color coincident with the consumption of acetate and sulfate and the production of Fe^{II}.

In the early phase, Fe^{II} began accumulating almost immediately in both AQDS+ and AQDS – bioreactors, with a significant step-wise increase at day 3 in the AQDS+ bioreactor (Fig 1). After one week, nearly 2 mM of Fe^{II} had accumulated in AQDS+ bioreactors compared to

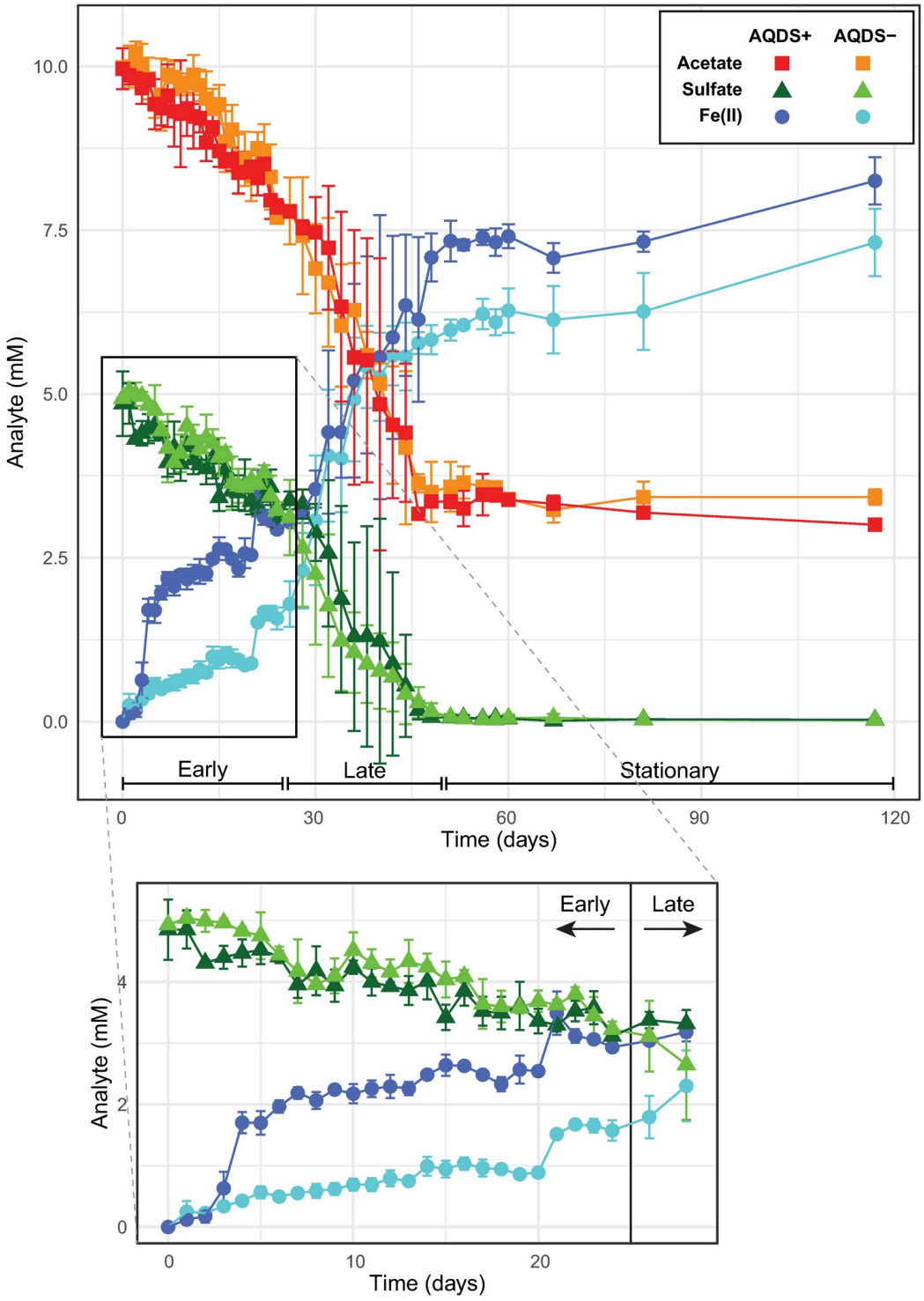

Fig 1. Analyte concentrations in bioreactors. Concentrations of total ferrous iron (Fe^{II}), acetate, and sulfate over time in AQDS–amended (AQDS+) and control bioreactors (AQDS–) with an expanded view of Fe^{II} and sulfate concentrations from 0–28 days.

https://doi.org/10.1371/journal.pone.0251883.g001

Table 1. Rates of Fe^{II} production and sulfate and acetate consumption.

		Fe^{II} production	Sulfate consumption	Acetate consumption
		rate	rate	rate
System	Phase[a]	mM day^{-1}	mM day^{-1}	mM day^{-1}
Without AQDS (AQDS-)	Early	0.056 ± 0.001[b]	-0.067 ± 0.006	-0.081 ± 0.008
	Late	0.308 ± 0.019	-0.196 ± 0.016	-0.203 ± 0.009
With AQDS (AQDS+)	Early	0.549 ± 0.147	-0.061 ± 0.005	-0.081 ± 0.004
	Late	0.228 ± 0.017	-0.203 ± 0.021	-0.224 ± 0.013

[a]Early and late phases as indicated in Fig 1.

[b]Rates (average ± standard error) were calculated by least-squares regression of data during the linear portion of the indicated phase.

https://doi.org/10.1371/journal.pone.0251883.t001

~0.5 mM in AQDS– systems, consistent with the higher rate of Fe^{II} production in the AQDS+ bioreactors (Table 1). The production of Fe^{II} was concomitant with the consumption of acetate. The depletion of sulfate began almost as soon as the production of Fe^{II} in both the AQDS+ and AQDS– bioreactors, with no significant difference in sulfate consumption rates observed between the two sets of reactors. During the early phase, the concentration of sulfate decreased from 5 mM to ~3.5 mM while the concentration of acetate decreased from 10 mM to ~8 mM (Fig 1).

The late phase was demarcated by a substantial increase in the rates of consumption of sulfate and acetate in both AQDS+ and AQDS– bioreactors, coincident with a significant increase in the rate of Fe^{II} production in the AQDS- bioreactors (Fig 1 and Table 1) and continued Fe^{II} production in the AQDS+ bioreactors (albeit at a slower rate than during the early phase). Over this phase of the experiment, the amount of Fe^{II} more than doubled from 3.0 mM to 8.3 mM in the AQDS+ experiments and increased from 1.6 to 7.3 in the AQDS– bioreactors. No significant difference in the rate of sulfate consumption was observed between AQDS+ and AQDS– reactors during this phase; given that sulfate (unlike Fe^{III} oxides) is a soluble electron acceptor, it is perhaps not surprising that the presence of the electron shuttle AQDS did not increase the rate of sulfate reduction. The consumption of acetate ceased and the production of Fe^{II} diminished when all the sulfate was consumed, leading to a quiescent stationary phase over the final 100 days of the experiment during which only marginal geochemical changes were observed. Approximately 3.5 mM of acetate remained in both the AQDS+ and AQDS – reactors. At the final measurement, the amount of Fe^{II} present in the AQDS+ bioreactors was 8.3±0.4 mM compared to 7.3±0.5 mM in the AQDS–bioreactors, with 3.4±0.1 mM of acetate remaining the AQDS+ bioreactors and 3.0±0.1 mM in the AQDS–bioreactors. Although Fe^{III} and sulfate reduction reactions consume protons (i.e., raise the pH), the pH of bioreactors remained well-buffered over the duration of the incubation, only increasing from 7.5 to ~7.8. No changes in Fe^{II}, acetate, and sulfate concentrations were observed in the sterile controls (S1 Fig in Supporting Information (S1 File)).

XAFS spectroscopy

The Fe transformations in the bioreactors were characterized in subsamples taken after 144 days of incubation. Fig 2A and 2B compare the XANES spectra of the bioreactors to the sterile control and to Fe^{II}/Fe^{III} standards. The sterile control shows the same edge position as the goethite standard, confirming that no Fe reduction occurred without inoculation. The edge position of the bioreactors samples is shifted in the direction of the Fe^{II} standard, which indicates partial reduction. Linear combination (LC) fits quantify the Fe^{II} content in the bioreators as 17% (±5%) of total solid-phase Fe (i.e., 5.2 mM Fe^{II}), which is significantly lower than the Fe^{II}

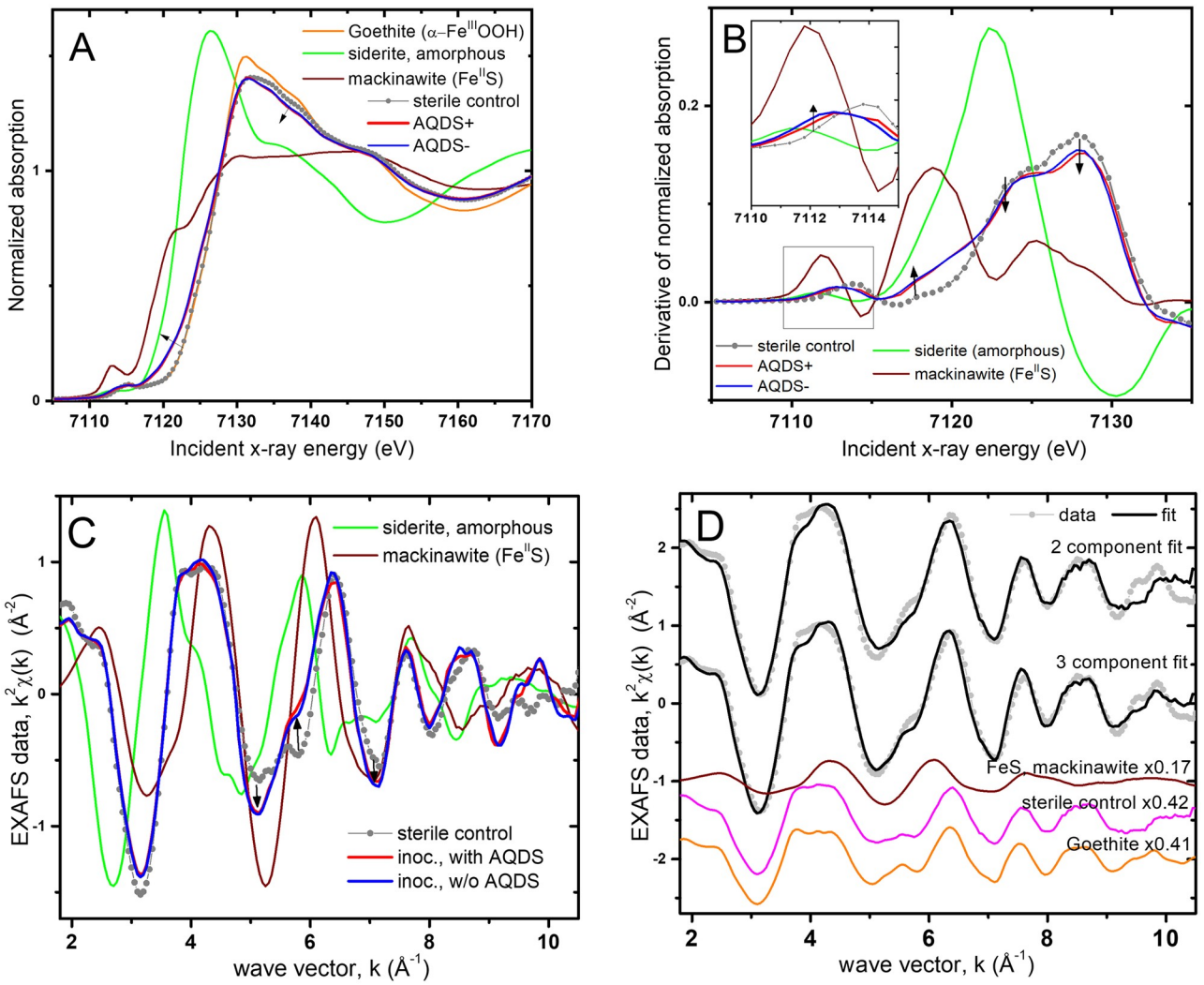

Fig 2. Fe XAFS analysis of bioreactor solids. Comparisons of XANES data from the bioreactors (with (AQDS+) and without AQDS (AQDS–)) to the sterile control and Fe^{II}/Fe^{III} standards. The lines corresponding to the AQDS+ and AQDS- bioreactors (red and blue) nearly overlap. A) XANES data. Arrows indicate the spectral shifts from Fe^{III} to Fe^{II} standards. B) Derivative of the spectra in A. Arrows point in the direction of the spectral shifts towards the $Fe^{II}S$ standard. Inset shows detail in the pre-edge region (box). C) EXAFS data. Arrows point in the direction of spectral shifts towards the $Fe^{II}S$ standard. D) LC fit of the data from the inoculated AQDS–bioreactors using two and three endmembers (the data for AQDS+ and AQDS – bioreactors are the same within measurement uncertainty). The weighted components in the best fit are offset for clarity. Mackinawite and the sterile control were the best fit components in both 2- and 3-component LC models. The fit range is 2-10 $Å^{-1}$ and the refined proportions are summarized in S1 Table in S1 File.

https://doi.org/10.1371/journal.pone.0251883.g002

concentrations measured in the acid extracts (8.3±0.4 mM in the AQDS+ bioreactors and 7.3 ±0.5 mM in the AQDS–bioreactors). Since both microcoms contained only 0.9 mM dissolved Fe^{II}, thee majority of the discrepancy between the Fe^{II} contents determined by XAFS and colorimetrically is likely due to an artifact of the acid extraction method [74] which can lead to an overestimation of Fe^{II} in systems containing sulfide and labile Fe^{III} oxides. The shape of the XANES features suggests FeS formation (Fig 2B), corroborated below by LC analysis of the EXAFS spectrum; additional details of the XANES analysis are presented in the SI.

The EXAFS spectra of the bioreactor solids are compared to the sterile control and to standards in Fig 2C. The AQDS+ and AQDS– bioreactors have identical EXAFS spectra, indicating that AQDS did not influence the final distribution of secondary mineralization products

(SMPs). The proportions of SMPs in the bioreactors were quantified by LC fits of the EXAFS data. Fits with 2- and 3-components showed that the spectral combination of the sterile control and FeS provided a significantly better fit to the data than with any of the other Fe^{II}-containing standards (Fig 2D, details in S1 File). The slight improvement of the fit with an additional goethite component suggests that the more labile oxides in the natural sienna starting phase are likely transformed first into reduced Fe^{II}, leaving an increased relative proportion of goethite in the Fe^{III} pool. Overall, the x-ray spectroscopy results indicate the formation of FeS in the inoculated reactors and quantify its proportion as approximately 18% of solid-phase Fe. Minor SMPs (<10% of solid-phase Fe) could not be resolved by the LC analysis.

Microbial community dynamics

The distinct "early" and "late" phases observed in the geochemical composition of the bioreactors were mirrored by changes in the composition of the microbial community. A corresponding shift over time in the microbial communities was observed in both the alpha and the beta diversity of the system. The alpha diversity, a measurement of the diversity of distinct microbial OTUs within a particular sample, here measured by both Shannon's and Simpson's indices of diversity, showed an initial sharp decrease followed by an overall increase (Fig 3). The alpha diversity decreased more rapidly in the AQDS+ bioreactors than in the AQDS− system, where the decline in diversity reached its nadir approximately one week after the AQDS+ system.

This distinction between early- and late-phase composition of the microbial community can also be seen in the NMDS plot of microbial communities from the bioreactors (Fig 4), where communities sampled at early time points cluster separately from those in the later phases. Based on the analysis of similarity metric (ANOSIM), the separation of early- from late-phase communities is statistically significant with an $R_{ANOSIM} = 0.684$ and a corresponding $p < 0.001\%$. A value of $R_{ANOSIM} > 0.75$ indicates that two groups of microbial communities are almost entirely distinct from one another [75]. Lower values ranging from 0.75 to 0.25 indicate the groups overlap to some degree, while values < 0.25 indicate very little difference in the average composition of the two groups being compared. In the early phase, the AQDS+ and AQDS–communities do not differ significantly with an R_{ANOSIM} value of only 0.102 ($p = 2.9\%$). Differences between the two treatments are much more distinct in the late phase, where $R_{ANOSIM} = 0.505$ ($p = 0.060\%$).

The steep decline in alpha diversity seen in Fig 3 corresponds with the onset of Fe^{II} production and the substantial increase between day 2 and day 4 of sequences belonging to the genus *Geobacter* (Fig 5). All currently known *Geobacter* isolates are capable of reducing Fe^{III} minerals [2]. Sequences classified as *Geobacter* accounted for only 2.5–3.0% of the total in both AQDS+ and AQDS–bioreactors on day 2, but that proportion increased to 79.0% by day 4 in AQDS+ bioreactors and 62.6% in AQDS–bioreactors. For the rest of the early phase of Fe^{II} production, *Geobacter* was the dominant taxonomic group, comprising 67.9% (AQDS+) and 46.7% (AQDS–) of the total taxonomic diversity, on average, prior to day 25. However, this dominance was more pronounced in the early phase of the AQDS+ bioreactors, where *Geobacter* sequences accounted for 56.1% of the total community compared to only 35.7% in AQDS–bioreactors. In addition to *Geobacter*, sequences most closely related to the dissimilatory metal-reducer *Albidiferax* were also abundant in the early phase. At day 2, *Albidiferax* sequences accounted for 36.6% of the total in AQDS+ bioreactors and 41.4% in AQDS–bioreactors. Only two days later, however, their share of the total had declined to 7.0% and 15.7%. *Albidiferax* sequences averaged only 16.2% and 10.9%, respectively, of the total relative abundance for the remainder of the early phase. *Albidiferax ferrireducens* (formerly *Rhodoferax ferrireducens*) is a

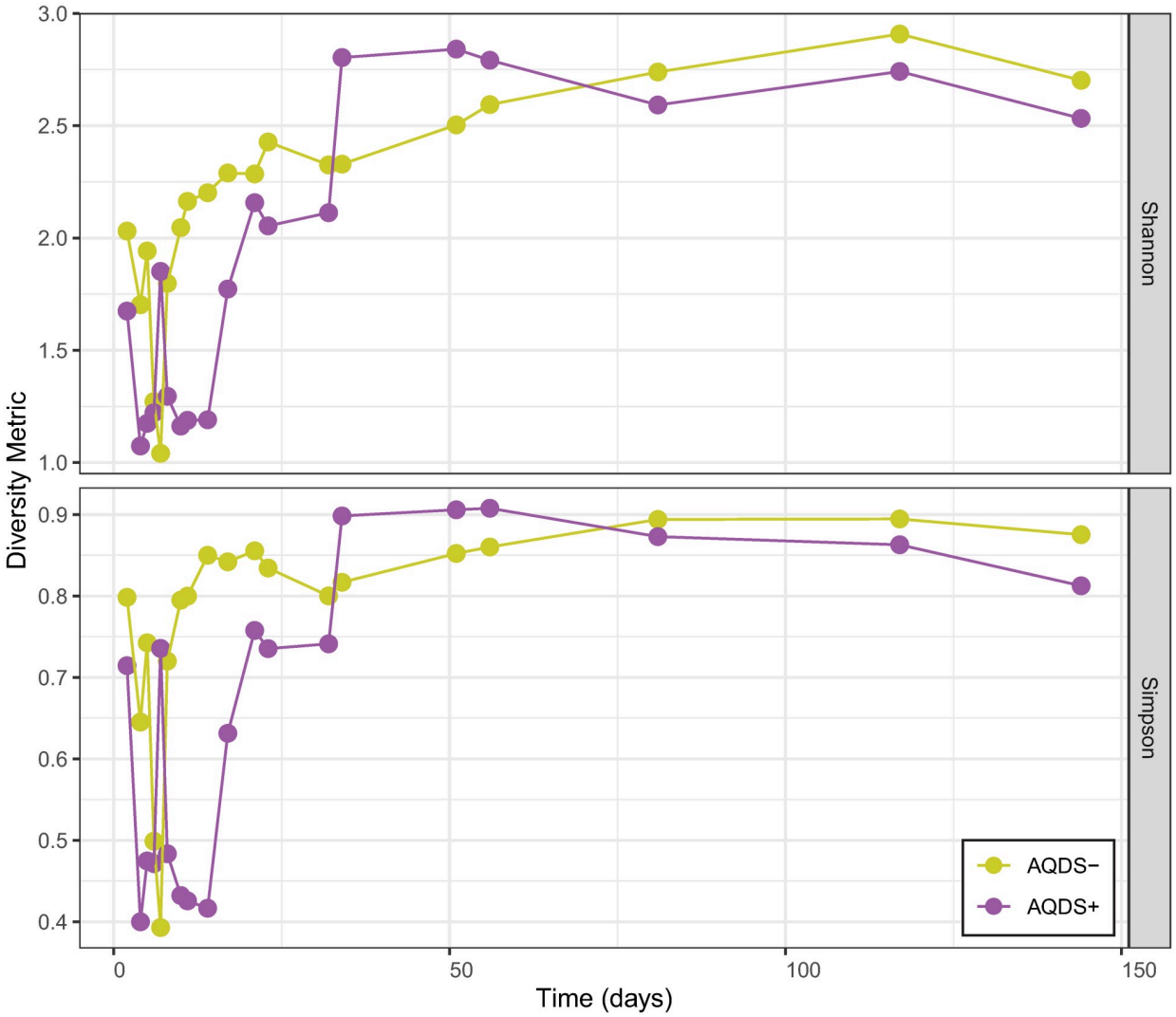

Fig 3. Changes in alpha diversity over time. Change over time in average alpha diversity as measured by the Shannon (top) and Simpson (bottom) indices during early and late phases of microbial community development in batch systems with (AQDS+) or without (AQDS–) added electron shuttle.

https://doi.org/10.1371/journal.pone.0251883.g003

member of the *Comamonadaceae* family that has been previously shown to reduce both Fe^{III} and Mn^{IV} but, interestingly, not AQDS [76].

In the late phase of the bioreactor experiments, the composition of the microbial community in both AQDS+ and AQDS–bioreactors shifted to one dominated by organisms most closely related to known sulfate-reducing bacteria. This is primarily due to a sharp increase in the relative abundance of sequences classified as *Desulfosporosinus* (Fig 5), a genus of known sulfate-reducing bacteria that have been observed to proliferate in organic C-amended soils and sediments from a variety of environments [56,77–82]. Sequences classified as this genus accounted for only 0.8–1.1% of all sequences in the early phase of the experiment, but their relative abundance increased sharply from 2.3% to 60.5% of all sequences in the AQDS+ experiments and from 3.1 to 46.4% in AQDS–between day 23 and day 32 of the experiments. *Desulfosporosinus* sequences remained the most abundant taxa in the late phase stage of the experiment, with an average relative abundance of 35.0% (AQDS+) and 33.2% (AQDS–)

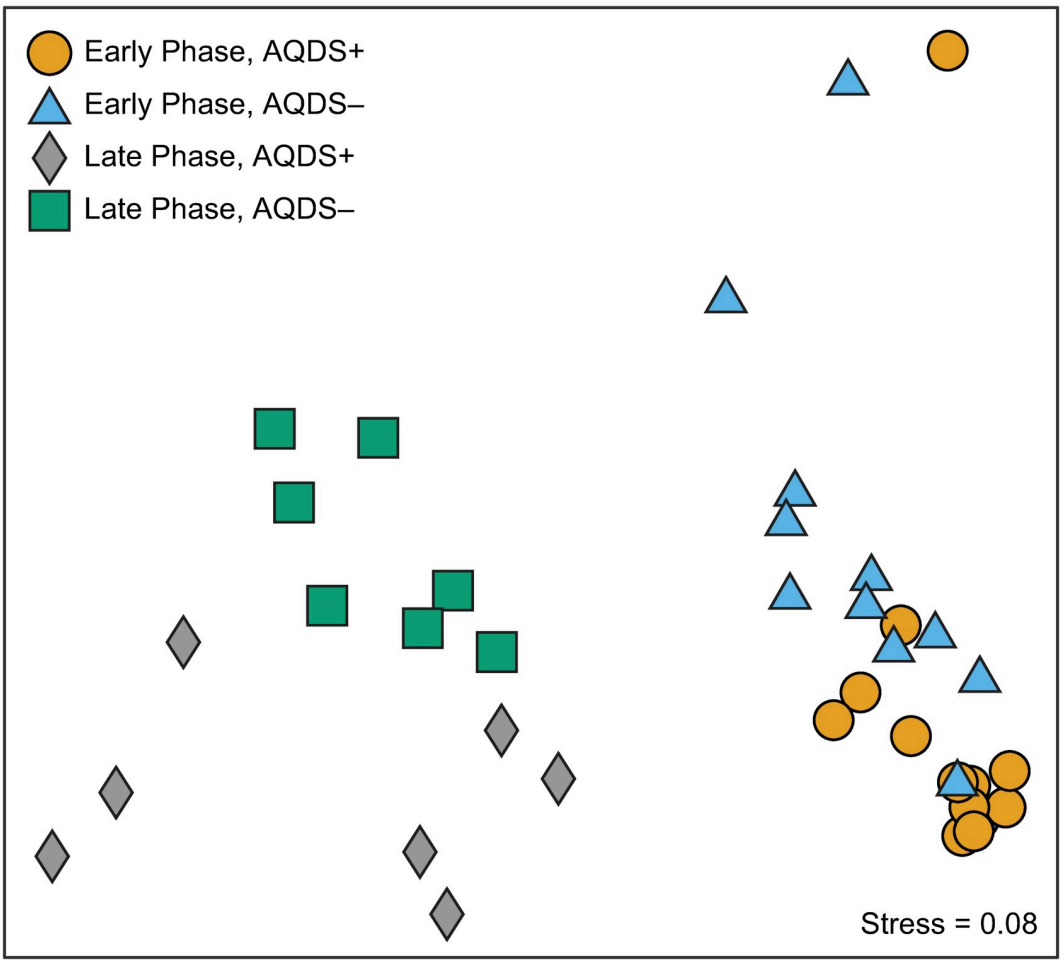

Fig 4. Nonmetric multidimensional scaling (NMDS) of microbial communities. Nonmetric multidimensional scaling (NMDS) of microbial communities in Fe^{III}-, sulfate-, and acetate-amended bioreactors over time according to the presence (AQDS+) or absence (AQDS–) of the electron shuttle AQDS.

https://doi.org/10.1371/journal.pone.0251883.g004

through day 144. While *Desulfosporosinus* sequences were the most abundant for taxa related to known sulfate reducers, sequences classified within the phylotype "SRB2" within the class *Thermoanaerobacterales* were present at an abundance ranging from 5.3–24.9% after day 51. While the phylogenetic placement of taxa within this class remains uncertain, some taxa within the group are associated with reductive S-cycling [83–85].

Comparisons of differentially abundant OTUs made using edgeR identified 9 OTUs that were significantly more or less abundant between the late-phase AQDS+ and AQDS–bioreactors (Fig 6). An OTU classified as genus *Dethiobacter*, a member of phylum *Clostridia* known to utilize thiosulfate, elemental sulfur and polysulfide as electron acceptors (but not sulfate), was considerably more abundant in the late-phase AQDS+ bioreactors compared to AQDS–. Conversely, the most differentially abundant OTU in the AQDS–bioreactors was most closely related to *Thermincola*, a Fe^{III}-reducing member of phylum *Clostridia*. Other differentially abundant OTUs include *Gracilibacter*, *Phyllobacterium*, and the SRB2 family of order *Thermoanaerobacterales*. OTUs classified as *Geobacter* and *Desulfosporosinus* were also more abundant in the AQDS+ bioreactors, although these particular OTUs were not the dominant OTUs responsible for most of the relative abundance of these particular taxa. The most differentially

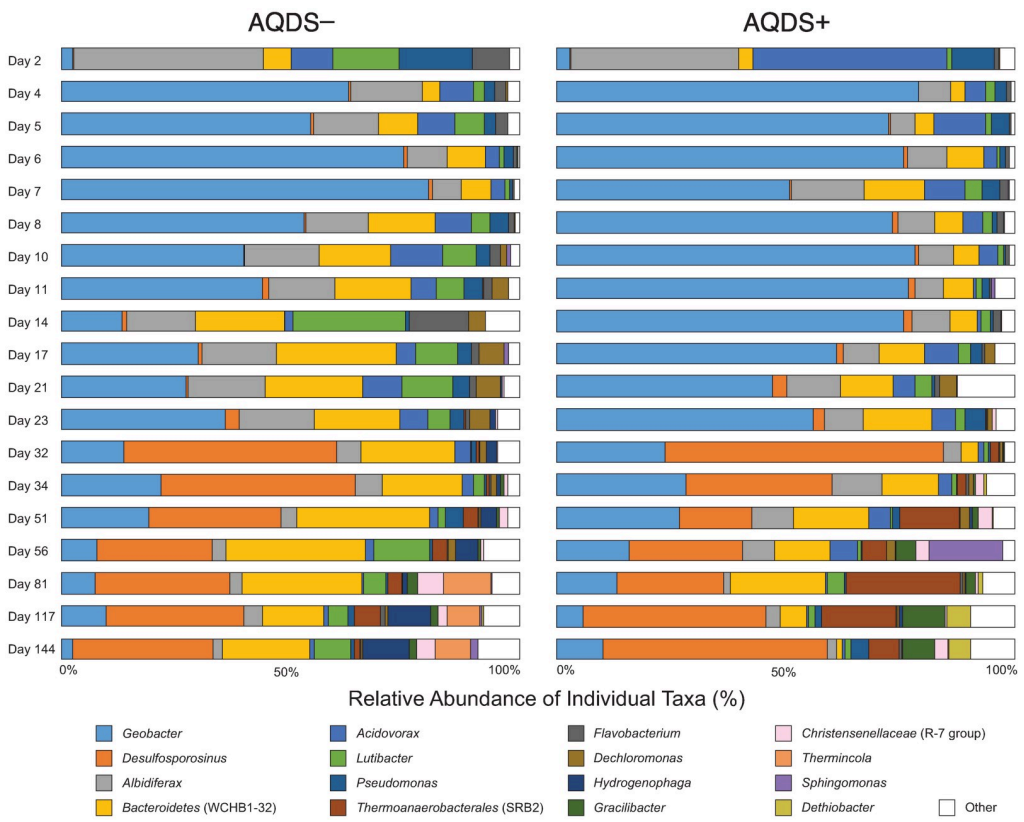

Fig 5. Changes in the relative abundance of microbial taxa over time. Comparison of the relative abundance of individual taxa detected by 16S rRNA gene amplicon sequencing in bioreactors amended with natural goethite, sulfate, and acetate in the presence (AQDS+) or absence (AQDS−) of the electron shuttle AQDS.

https://doi.org/10.1371/journal.pone.0251883.g005

abundant *Geobacter* OTU is OTU-7, which was more than 10 times as abundant in the late-phase of AQDS+ bioreactors than it was in those without AQDS. This particular OTU was barely detectable in the early, *Geobacter*-dominated phase of the AQDS+ treatment but grew to become the dominant *Geobacter* OTU over the late, *Desulfosporosinus*-dominated phase (Fig 7).

Discussion

The addition of the electron shuttle AQDS did increase the initial rate of Fe^{III} reduction (Fig 1 and Table 1); however, it had little effect on the composition of the microbial community during this phase (Fig 5). The increase in Fe^{II} in both AQDS+ and AQDS–bioreactors corresponded directly to an increase in the relative abundance of sequences classified as *Albidiferax* and *Geobacter*. A single OTU dominated the *Geobacter* in the AQDS–bioreactors throughout the experiment and in the AQDS+ bioreactors through day 56 (Fig 7). Both *Albidiferax* and *Geobacter* are known to reduce ferric minerals like the goethite present in the natural sienna amendment. *Geobacter* in particular has been shown to predominate in sedimentary environments where Fe^{III} reduction is occurring [86–91], typically in response to acetate biostimulation [56,92–97]. This pattern is well-established, as *Geobacter* blooms have been observed in Fe^{III}- and acetate-amended bioreactors using material from rice paddies [98], marshes [99], and aquifer sediment [100,101]. *Geobacter* has also been enriched in acetate-amended experimental systems where AQDS (not Fe^{III}) was added as the sole electron acceptor [102]. Some

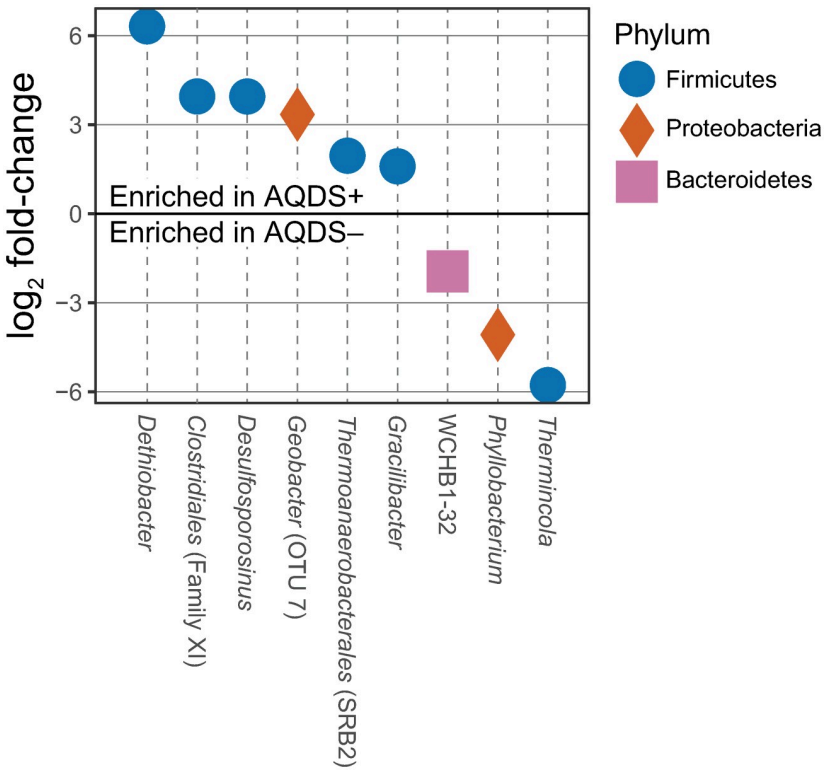

Fig 6. Comparisons of OTUs significantly more or less abundant between the late-phase AQDS+ and AQDS– bioreactors. Differentially-abundant OTUs in AQDS+ and AQDS–bioreactors as determined by edgeR. OTUs with a positive log2-fold change value are more relatively abundant in AQDS+ bioreactors, while those with a negative value are more relatively abundant in AQDS–bioreactors.

https://doi.org/10.1371/journal.pone.0251883.g006

other taxa (e.g., *Acidovorax*) were abundant at day 2, but these were quickly overtaken in dominance by *Geobacter*.

Given the diversity of organisms capable of reducing synthetic (e.g., AQDS) and naturally occurring quinones (e.g., humic substances) [44], we had hypothesized that the presence of AQDS would lead to greater microbial diversity in the AQDS+ bioreactors during Fe^{III} reduction due to recruitment of non-metal-reducing, quinone-respiring organisms. However, this was not the case under our experimental conditions. In both AQDS+ and AQDS–bioreactors diversity declined at the onset of Fe^{II} production, with sequences classified as *Geobacter* becoming more abundant. Indeed, *Geobacter* were even more dominant in the AQDS+ systems than in AQDS–; which in retrospect is perhaps not unexpected given their ability to use both Fe^{III} and AQDS as terminal electron acceptors for anaerobic respiration [2]. A similar enhancement in *Geobacter* abundance was reported by Rowland et al. [100] in microcosm studies where sediments were amended with acetate alone or acetate and AQDS (50 μM; an order of magnitude lower AQDS concentration than in our study) and by Chen et al [103] where the relative abundance of *Geobacter* in rice paddy soil incubations increased with increasing AQDS concentration. It is possible that AQDS may be toxic to some members of the Fe^{III}-reducing community, potentially decreasing diversity. Direct evidence of the potential toxicity of AQDS to bacteria is lacking; however, circumstantial evidence suggests that AQDS toxicity is not likely to be an issue in our systems containing such low (100 μM) concentrations of the quinone molecule. In acetate-amended sediment incubations, lower Fe^{II} concentrations were observed in systems containing 250 μM AQDS compared with 50 μM, the next lowest

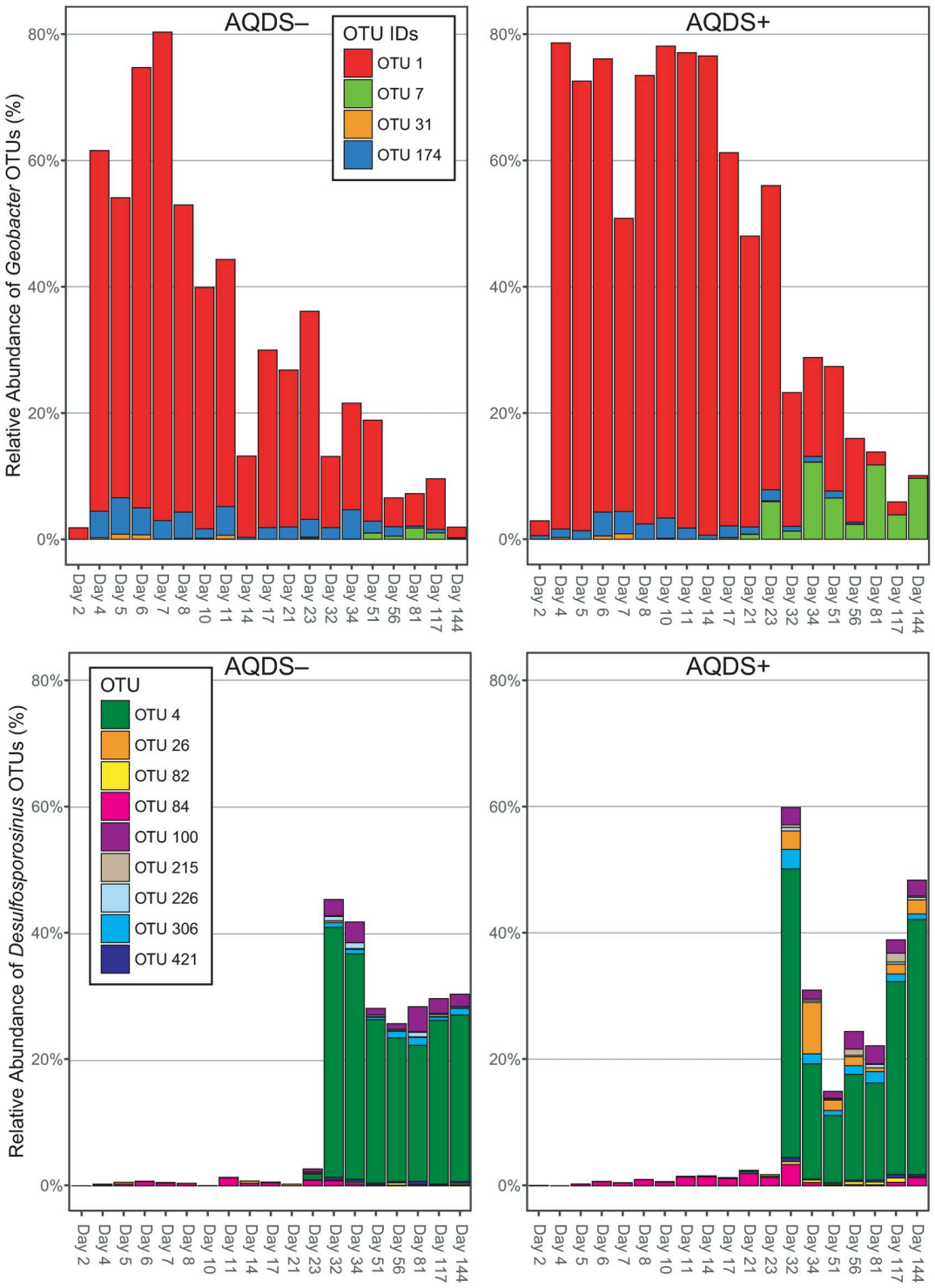

Fig 7. Relative abundance of *Geobacter* and *Desulfosporosinus*. Relative abundance of operational taxonomic units (OTUs) classified as *Geobacter* or *Desulfosporosinus* in AQDS+ and AQDS–bioreactors.

https://doi.org/10.1371/journal.pone.0251883.g007

concentration examined [21]. However, AQDS concentrations as high as 20 mM showed no inhibition of Fe^{II} production relative to concentrations as low as 10 μM in rice paddy soil incubations [103]. Furthermore, pure culture studies with *Geobacter sulfurreducens* and *Shewanella putrefaciens* CN32 showed no inhibition of Fe^{II} production with 500 μM and 1000 μM AQDS, respectively [20,104].

Similar to the trajectory observed following acetate injection in a uranium-contaminated aquifer in Rifle, Colorado [56] (the same location from which the sediment used to inoculate the bioreactors was obtained), the initial bloom of *Geobacter* was followed by a period of sulfate reduction and the increased relative abundance of sequences associated with sulfate-reducing bacteria. At both Rifle and in our experiment, the most abundant taxa associated with sulfate reduction were of the genus *Desulfosporosinus*. Initially at less than <1% of the total community in these systems, *Desulfosporosinus* sequences eventually came to dominate the microbial community during the latter stages of the experiment, where they accounted for roughly one-third of all sequences in both the AQDS+ and AQDS–bioreactors (Fig 5). As with the *Geobacter* OTUs, a single *Desulfosporosinus* OTU dominated in both AQDS+ and AQDS–bioreactors (Fig 7). In addition to the bioreactors in this study, as well as an earlier study from our group [105], *Desulfosporosinus* have previously been found in acetate-amended sediments [78,106,107].

The preponderance of *Desulfosporosinus* in these acetate-amended systems is perhaps unexpected given the inability of all previously cultivated *Desulfosporosinus* spp. to couple acetate oxidation to dissimilatory sulfate reduction [108–118]. However, the increase in the relative abundance of *Desulfosporosinus* in our bioreactors was coincident with a sharp increase in the rate of sulfate consumption (Fig 1 and Table 1), suggesting that they are active contributors to sulfate reduction in this system. *G. sulfurreducens* can oxidize acetate by syntrophic association with hydrogen-oxidizing anaerobic partners [119,120] and many *Desulfosporosinus* spp. can use H_2 as an electron donor for dissimilatory sulfate reduction [109,110,114,116,118,121] suggesting the possibility for sulfate reduction via a syntrophic association between *Geobacter* and *Desulfosporosinus*.

Of particular note is that the majority of Fe^{II} production actually occurred during the "sulfate-reducing" latter phase of the experiment. During the early phase of the experiment dominated by *Albidiferax* and *Geobacter*, <10% of the total amount of Fe^{III} added was reduced. Indeed, 64% and 78% of the total amount of Fe^{II} produced occurred during the "sulfate-reducing" phase in AQDS+ and AQDS–bioreactors, respectively, likely driven by the reduction of Fe^{III} by the sulfide produced by *Desulfosporosinus* and other SRB [122]. These results are consistent with recent findings highlighting the potential importance of sulfur-driven reactions in the biogeochemical cycling of iron in sedimentary environments. Because iron reduction is strongly pH-dependent, experimental and modeling evidence suggests that under sulfidic, alkaline conditions, Fe^{III} reduction by metal-reducing bacteria likely proceeds primarily via an electron shuttling pathway mediated by S^0 [31]. Even under circumneutral conditions, laboratory and field studies suggest that sulfur cycling can play a significant role in Fe^{III} reduction in freshwater and marine environments [122–125].

These results call into question the paradigm of parsing out geomicrobiological reactions into "iron-reducing" and "sulfate-reducing" phases. This traditional conception of terminal electron accepting processes in the subsurface, while long-established (e.g., [126]), has increasingly been called into question by both theoretical and experimental observations in both the field and laboratory. Iron reduction and sulfate reduction have frequently been observed to co-occur in sedimentary environments [86,87,127–129], and modeling results predict that the co-occurrence of these processes may even benefit both groups [130,131]. In our results, sulfate reduction began essentially consequent with iron reduction. While some of the sulfate

may have been consumed by assimilatory sulfate reduction during the growth of other organisms, this is unlikely as there was no difference in the rate of sulfate consumption between AQDS+ and AQDS–systems. If the growth of iron reducers was responsible for the decrease in the concentration of sulfate, the rate of sulfate consumption would have been greater during the early phase in AQDS+ bioreactors. While initially higher rates of growth, particularly in the presence of electron shuttles, may give iron reducers an early advantage under growth-stimulating conditions, such dynamics may ultimately bear little resemblance to the processes that occur in most aquifers.

Supporting information

S1 File. Supporting information on geochemical conditions in the sterile controls and Fe mineralogy and XAFS analysis. Fe^{II}, acetate, and sulfate concentrations over time in the sterile controls as well as a detailed description of the characterization of Fe mineralogy in natural sienna and details of the XAFS analysis of bioreactor solids.
(DOCX)

Acknowledgments

We thank Kenneth Williams and Philip Long (Lawrence Berkeley National Laboratory) for the Rifle Integrated Field Research Challenge site sediment sample; the Materials Research Collaborative Access Team (MRCAT) beamline staff for assistance during data collection; and the anonymous reviewers for their thoughtful comments.

Author Contributions

Conceptualization: Kenneth M. Kemner, Edward J. O'Loughlin.

Data curation: Theodore M. Flynn, Dionysios A. Antonopoulos, Kelly A. Skinner.

Formal analysis: Theodore M. Flynn, Dionysios A. Antonopoulos, Kelly A. Skinner, Jennifer M. Brulc, Eric Johnston, Maxim I. Boyanov, Man Jae Kwon, Edward J. O'Loughlin.

Funding acquisition: Kenneth M. Kemner.

Investigation: Kelly A. Skinner, Maxim I. Boyanov, Man Jae Kwon, Edward J. O'Loughlin.

Methodology: Dionysios A. Antonopoulos, Maxim I. Boyanov, Edward J. O'Loughlin.

Project administration: Kenneth M. Kemner.

Supervision: Kenneth M. Kemner, Edward J. O'Loughlin.

Writing – original draft: Theodore M. Flynn, Dionysios A. Antonopoulos, Kelly A. Skinner, Maxim I. Boyanov, Edward J. O'Loughlin.

Writing – review & editing: Theodore M. Flynn, Dionysios A. Antonopoulos, Kelly A. Skinner, Eric Johnston, Maxim I. Boyanov, Man Jae Kwon, Kenneth M. Kemner, Edward J. O'Loughlin.

References

1. Melton ED, Swanner ED, Behrens S, Schmidt C, Kappler A. The interplay of microbially mediated and abiotic reactions in the biogeochemical Fe cycle. Nature Reviews Microbiology. 2014. Epub 2014/10/21. https://doi.org/10.1038/nrmicro3347 PMID: 25329406.

2. Lovley D. Dissimilatory Fe(III)- and Mn(IV)-reducing prokaryotes. In: Dworkin M, editor. The Prokaryotes—Prokaryotic Physiology and Biochemistry. Berlin Heidelburg: Springer-Verlag; 2013. p. 287–308.
3. Weber KA, Urrutia MM, Churchill PF, Kukkadapu RK, Roden EE. Anaerobic redox cycling of iron by freshwater sediment microorganisms. Environ Microbiol. 2006; 8(1):100–13. Epub 2005/12/14. https://doi.org/10.1111/j.1462-2920.2005.00873.x PMID: 16343326.
4. Kirk MF, Crossey LJ, Takacs-Vesbach C, Newell DL, Bowman RS. Influence of upwelling saline groundwater on iron and manganese cycling in the Rio Grande floodplain aquifer. Applied Geochemistry. 2009; 24(3):426–37. https://doi.org/10.1016/j.apgeochem.2008.12.022
5. Fendorf S, Michael HA, van Geen A. Spatial and temporal variations of groundwater arsenic in South and Southeast Asia. Science. 2010; 328(5982):1123–7. Epub 2010/05/29. https://doi.org/10.1126/science.1172974 PMID: 20508123.
6. Fredrickson JK, Zachara JM, Kennedy DW, Dong H, Onstott TC, Hinman NW, et al. Biogenic iron mineralization accompanying the dissimilatory reduction of hydrous ferric oxide by a groundwater bacterium. Geochim Cosmochim Acta. 1998; 62(19/20):3239–57.
7. Dong H, Fredrickson JK, Kennedy DW, Zachara JM, Kukkadapu RK, Onstott TC. Mineral transformation associated with the microbial reduction of magnetite. Chemical Geology. 2000; 169(3–4):299–318. https://doi.org/10.1016/S0009-2541(00)00210-2
8. Hansel CM, Benner SG, Neiss J, Dohnalkova A, Kukkadapu RK, Fendorf S. Secondary mineralization pathways induced by dissimilatory iron reduction of ferrihydrite under advective flow. Geochim Cosmochim Acta. 2003; 67(16):2977–92. https://doi.org/10.1016/S0016-7037(03)00276-X
9. Chacon N, Silver WL, Dubinsky EA, Cusack DF. Iron reduction and soil phosphorus solubilization in humid tropical forests soils: The roles of labile carbon pools and an electron shuttle compound. Biogeochem. 2006; 78(1):67–84. https://doi.org/10.1007/s10533-005-2343-3
10. Lovley DR, Anderson RT. Influence of dissimilatory metal reduction on the fate of organic and metal contaminants in the subsurface. Hydrogeology Journal. 2000; 8:77–88.
11. Shi L, Dong H, Reguera G, Beyenal H, Lu A, Liu J, et al. Extracellular electron transfer mechanisms between microorganisms and minerals. Nature Reviews Microbiology. 2016; 14(10):651–62. Epub 2016/08/31. https://doi.org/10.1038/nrmicro.2016.93 PMID: 27573579.
12. Shi L, Richardson DJ, Wang Z, Kerisit SN, Rosso KM, Zachara JM, et al. The roles of outer membrane cytochromes of *Shewanella* and *Geobacter* in extracellular electron transfer. Environmental Microbiology Reports. 2009; 1(4):220–7. https://doi.org/10.1111/j.1758-2229.2009.00035.x PMID: 23765850
13. Gorby YA, Yanina S, McLean JS, Rosso KM, Moyles D, Dohnalkova A, et al. Electrically conductive bacterial nanowires produced by *Shewanella oneidensis* strain MR-1 and other microorganisms. Proc Natl Acad Sci. 2006; 103(30):11358–63. Epub 2006/07/20. https://doi.org/10.1073/pnas.0604517103 PMID: 16849424.
14. Reguera G, McCarthy KD, Metha T, Nicoll JS, Tuominen MT, Lovley DR. Extracellular electron transfer via microbial nanowires. Nature. 2005; 435(7045):1098–101. Epub 2005/06/24. https://doi.org/10.1038/nature03661 PMID: 15973408.
15. Lovley DR. Electrically conductive pili: Biological function and potential applications in electronics. Current Opinion in Electrochemistry. 2017; 4(1):190–8. https://doi.org/10.1016/j.coelec.2017.08.015
16. Malvankar NS, Vargas M, Nevin K, Tremblay PL, Evans-Lutterodt K, Nykypanchuk D, et al. Structural basis for metallic-like conductivity in microbial nanowires. mBio. 2015; 6(2):e00084. Epub 2015/03/05. https://doi.org/10.1128/mBio.00084-15 PMID: 25736881.
17. Subramanian P, Pirbadian S, El-Naggar MY, Jensen GJ. Ultrastructure of Shewanella oneidensis MR-1 nanowires revealed by electron cryotomography. Proceedings of the National Academy of Sciences of the United States of America. 2018; 115(14):E3246–E55. Epub 2018/03/21. https://doi.org/10.1073/pnas.1718810115 PMID: 29555764.
18. Nevin KP, Lovley DR. Mechanisms for Fe(III) oxide reduction in sedimentary environments. Geomicrobiol J. 2002; 19:141–59.
19. Taillefert M, Beckler JS, Carey E, Burns JL, Fennessey CM, DiChristina TJ. *Shewanella putrefaciens* produces an Fe(III)-solubilizing organic ligand during anaerobic respiration on insoluble Fe(III) oxides. Journal of Inorganic Biochemistry. 2007; 101(11–12):1760–7. Epub 2007/09/04. https://doi.org/10.1016/j.jinorgbio.2007.07.020 PMID: 17765315.
20. O'Loughlin EJ. Effects of electron transfer mediators on the biodegradation of lepidocrocite (g-FeOOH) by *Shewanella putrefaciens* CN32. Environ Sci Technol. 2008; 42(18):6876–82. https://doi.org/10.1021/es800686d PMID: 18853803
21. Nevin KP, Lovley DR. Potential for nonenzymatic reduction of Fe(III) via electron shuttling in subsurface sediments. Environ Sci Technol. 2000; 34(12):2472–8. https://doi.org/10.1021/Es991181b

22. Newman DK, Kolter R. A role for excreted quinones in extracellular electron transfer. Nature. 2000; 405(6782):94–7. Epub 2000/05/16. https://doi.org/10.1038/35011098 PMID: 10811225.

23. Nevin KP, Lovley DR. Mechanisms for accessing insoluble Fe(III) oxide during dissimilatory Fe(III) reduction by *Geothrix fermentans*. Appl Environ Microbiol. 2002; 68(5):2294–9. Epub 2002/04/27. https://doi.org/10.1128/aem.68.5.2294-2299.2002 PMID: 11976100.

24. Turick CE, Tisa LS, Caccavo F, Jr. Melanin production and use as a soluble electron shuttle for Fe(III) oxide reduction and as a terminal electron acceptor by *Shewanella alga* BrY. Appl Environ Microbiol. 2002; 68(5):2436–44. https://doi.org/10.1128/aem.68.5.2436-2444.2002 PMID: 11976119

25. Doong R-a, Schink B. Cysteine-mediated reductive dissolution of poorly crystalline iron(III) oxides by *Geobacter sulfurreducens*. Environ Sci Technol. 2002; 36(13):2939–45. https://doi.org/10.1021/es0102235 PMID: 12144271

26. Hernandez ME, Kappler A, Newman DK. Phenazines and other redox-active antibiotics promote microbial mineral reduction. Appl Environ Microbiol. 2004; 70(2):921–8. Epub 2004/02/10. https://doi.org/10.1128/aem.70.2.921-928.2004 PMID: 14766572.

27. Straub KL, Schink B. Ferrihydrite-dependent growth of *Sulfurospirillum deleyianum* through electron transfer via sulfur cycling. Appl Environ Microbiol. 2004; 70(10):5744–9. https://doi.org/10.1128/AEM.70.10.5744-5749.2004 PMID: 15466509

28. von Canstein H, Ogawa J, Shimizu S, Lloyd JR. Secretion of flavins by *Shewanella* species and their role in extracellular electron transfer. Appl Environ Microbiol. 2008; 74(3):615–23. https://doi.org/10.1128/AEM.01387-07 PMID: 18065612

29. Marsili E, Baron DB, Shikhare ID, Coursolle D, Gralnick JA, Bond DR. *Shewanella* secretes flavins that mediate extracellular electron transfer. Proc Natl Acad Sci. 2008; 105(10):3968–73. https://doi.org/10.1073/pnas.0710525105 PMID: 18316736

30. Wolf M, Kappler A, Jiang J, Meckenstock RU. Effects of humic substances at low concentrations on ferrihydrite reduction by *Geobacter metallireducens*. Environ Sci Technol. 2009; 43(15):5679–85. https://doi.org/10.1021/es803647r PMID: 19731662

31. Flynn TM, O'Loughlin EJ, Mishra B, DiChristina TJ, Kemner KM. Sulfur-mediated electron shuttling during bacterial iron reduction. Science. 2014; 344(6187):1039–42. https://doi.org/10.1126/science.1252066 PMID: 24789972

32. Lovley DR, Coates JD, Blunt-Harris EL, Phillips EJP, Woodward JC. Humic-substances as electron acceptors for microbial respiration. Nature. 1996; 382(6590):445–8. https://doi.org/10.1038/382445a0

33. Royer RA, Burgos WD, Fisher AS, Jeon B-H, Unz RF, Dempsey BA. Enhancement of hematite bioreduction by natural organic matter. Environ Sci Technol. 2002; 36(13):2897–904. Epub 2002/07/30. https://doi.org/10.1021/es015735y PMID: 12144265.

34. Jiang J, Kappler A. Kinetics of microbial and chemical reduction of humic substances: Implications for electron shuttling. Environ Sci Technol. 2008; 42(10):3563–9. Epub 2008/06/13. https://doi.org/10.1021/es7023803 PMID: 18546690.

35. Roden EE, Kappler A, Bauer I, Jiang J, Paul A, Stoesser R, et al. Extracellular electron transfer through microbial reduction of solid-phase humic substances. Nature Geosciences. 2010; 3(6):417–21.

36. Scott DT, McKnight DM, Blunt-Harris EL, Kolesar SE, Lovley DR. Quinone moieties act as electron acceptors in the reduction of humic substances by humics-reducing microorganisms. Environ Sci Technol. 1998; 32:2984–9.

37. Klapper L, McKnight DM, Fulton JR, Blunt-Harris EL, Nevin KP, Lovley DR, et al. Fulvic acid oxidation state detection using fluorescence spectroscopy. Environ Sci Technol. 2002; 36(14):3170–5. https://doi.org/10.1021/es0109702 PMID: 12141500

38. Nurmi JT, Tratnyek PG. Electrochemical properties of natural organic matter (NOM), fractions of NOM, and model biogeochemical electron shuttles. Environ Sci Technol. 2002; 36(4):617–24. https://doi.org/10.1021/es0110731 PMID: 11878375

39. Struyk Z, Sposito G. Redox properties of standard humic acids. Geoderma. 2001; 102:329–46.

40. Bauer M, Heitmann T, Macalady DL, Blodau C. Electron transfer capacities and reaction kinetics of peat dissolved organic matter. Environ Sci Technol. 2007; 41(1):139–45. https://doi.org/10.1021/es061323j PMID: 17265939

41. Ratasuk N, Nanny MA. Characterization and quantification of reversible redox sites in humic substances. Environ Sci Technol. 2007; 41(22):7844–50. Epub 2007/12/14. https://doi.org/10.1021/es071389u PMID: 18075097.

42. Aeschbacher M, Vergari D, Schwarzenbach RP, Sander M. Electrochemical analysis of proton and electron transfer equilibria of the reducible moieties in humic acids. Environ Sci Technol. 2011; 45(19):8385–94. Epub 2011/08/10. https://doi.org/10.1021/es201981g PMID: 21823669.

43. Tratnyek PG, Macalady DL. Abiotic reductions of nitro aromatic pesticides in anaerobic laboratory systems. J Agric Food Chem. 1989; 37(1):248–54. https://doi.org/10.1021/Jf00085a058

44. Field JA, Cervantes FJ. Microbial redox reactions mediated by humics and structurally related quinones. In: Perminova IV, Hatfield K, Hertkorn N, editors. Use of humic substances to remediate polluted environments: From theory to practice. NATO Science Series: IV: Earth and Environmental Sciences. 52. Dordrecht: Springer; 2005. p. 343–52.

45. Glasser NR, Saunders SH, Newman DK. The colorful world of extracellular electron shuttles. Annu Rev Microbiol. 2017; 71(1):731–51. Epub 2017/07/22. https://doi.org/10.1146/annurev-micro-090816-093913 PMID: 28731847.

46. Benz M, Schink B, Brune A. Humic acid reduction by *Propionibacterium freudenreichii* and other fermenting bacteria. Appl Environ Microbiol. 1998; 64(11):4507–12. https://doi.org/10.1128/AEM.64.11.4507-4512.1998 PMID: 9797315

47. Lovley DR, Kashefi K, Vargas M, Tor JM, Blunt-Harris EL. Reduction of humic substances and Fe(III) by hyperthermophylic microorganisms. Chemical Geology. 2000; 169:289–98.

48. Luijten MLGC, Weelink SAB, Godschalk B, Langenhoff AAM, van Eekert MHA, Schraa G, et al. Anaerobic reduction and oxidation of quinone moieties and the reduction of oxidized metals by halorespiring and realted organisms. FEMS Microbiology Ecology. 2004; 49:145–50. https://doi.org/10.1016/j.femsec.2004.01.015 PMID: 19712392

49. McKinlay JP, Zeikus JG. Extracellular iron reduction is mediated in part by neutral red and hydrogenase in *Escherichia coli*. Appl Environ Microbiol. 2004; 70(6):3467–74. https://doi.org/10.1128/AEM.70.6.3467-3474.2004 PMID: 15184145

50. Coates JD, Ellis DJ, Blunt-Harris EL, Gaw CV, Roden EE, Lovley DR. Recovery of humic-reducing bacteria from a diversity of environments. Appl Environ Microbiol. 1998; 64(4):1504–9. https://doi.org/10.1128/AEM.64.4.1504-1509.1998 PMID: 9546186

51. Nevin KP, Lovley DR. Lack of production of electron-shuttling compounds or solubilization of Fe(III) during reduction of insoluble Fe(III) oxide by *Geobacter metallireducens*. Appl Environ Microbiol. 2000; 66(5):2248–51. Epub 2000/05/02. https://doi.org/10.1128/aem.66.5.2248-2251.2000 PMID: 10788411.

52. Finneran KT, Anderson RT, Nevin KP, Lovley DR. Potential for bioremediation of uranium-contaminated aquifers with microbial U(VI) reduction. Soil and Sediment Contamination. 2002; 11(3):339–57. https://doi.org/10.1080/20025891106781

53. Kappler A, Benz M, Schink B, Brune A. Electron shuttling via humic acids in microbial iron(III) reduction in a freshwater sediment. FEMS MIcrobiology Ecology. 2004; 47(1):85–92. Epub 2004/01/01. https://doi.org/10.1016/S0168-6496(03)00245-9 PMID: 19712349.

54. Peretyazhko T, Sposito G. Iron(III) reduction and phosphorous solubilization in humid tropical forest soils. Geochim Cosmochim Acta. 2005; 69(14):3643–52.

55. Rakshit S, Uchimiya M, Sposito G. Iron(III) bioreduction in soil in the presence of added humic substances. Soil Science Society of America Journal. 2009; 73(1):65–71. https://doi.org/10.2136/sssaj2007.0418

56. Anderson RT, Vrionis HA, Ortiz-Bernad I, Resch CT, Long PE, Dayvault R, et al. Stimulating the in situ activity of *Geobacter* species to remove uranium from the groundwater of a uranium-contaminated aquifer. Appl Environ Microbiol. 2003; 69(10):5884–91. Epub 2003/10/09. https://doi.org/10.1128/aem.69.10.5884-5891.2003 PMID: 14532040.

57. Fox PM, Davis JA, Hay MB, Conrad ME, Campbell KM, Williams KH, et al. Rate-limited U(VI) desorption during a small-scale tracer test in a heterogeneous uranium-contaminated aquifer. Water Resources Research. 2012; 48(5). https://doi.org/10.1029/2011wr011472

58. Stookey LL. Ferrozine-A new spectrophotometric reagent for iron. ANalytical Chemistry. 1970; 42 (7):779–81. https://doi.org/10.1021/ac60289a016

59. Sørensen J. Reduction of ferric iron in anaerobic, marine sediment and interaction with reduction of nitrate and sulfate. Appl Environ Microbiol. 1982; 43(2):319–24. https://doi.org/10.1128/AEM.43.2.319-324.1982 PMID: 16345937

60. Kropf AJ, Katsoudas J, Chattopadhyay S, Shibata T, Lang EA, Zyryanov VN, et al. The new MRCAT (Sector 10) bending magnet beamline at the Advanced Photon Source. AIP Conference Proceedings. 2010; 1234:299–302. https://doi.org/10.1063/1.3463194

61. Kemner KM, Kelly SD. Synchrotron-based techniques for monitoring metal transformation. In: Hurst CJ, editor. Manual of Environmental Microbiology. Third ed. Washington, DC: ASM Press; 2007. p. 1183–94.

62. Boyanov MI, Kemner KM. Application of synchrotron x-ray absorption spectroscopy and microscopy techniques to the study of biogeochemical processes. In: Kenney JPL, Veeramani H, Alessi DS,

editors. Analytical Geomicrobiology: A Handbook of Instrumental Techniques: Cambridge University Press; 2019. p. 238–61.

63. O'Loughlin EJ, Kelly SD, Csencsits R, Cook RE, Kemner KM. Reduction of uranium(VI) by mixed iron (II)/iron(III) hydroxide (green rust): Formation of UO_2 nanoparticles. Environ Sci Technol. 2003; 37 (4):721–7. https://doi.org/10.1021/es0208409 PMID: 12636270

64. Smith PK, Krohn RI, Hermanson GT, Mallia AK, Gartner FH, Provenzano MD, et al. Measurement of protein using bicinchoninic acid. Analytical Biochemistry. 1985; 150:76–85. https://doi.org/10.1016/0003-2697(85)90442-7 PMID: 3843705

65. Cole JR, Wang Q, Fish J, Chai B, Farris RJ, Kulam SA, et al. The Ribosomal Database Project: Improved alignments and new tools for rRNA analysis. Nucleic Acids Research. 2009; 37(Database issue):D141–D5. https://doi.org/10.1093/nar/gkn879 PMID: 19004872

66. Caporaso JG, Kuczynski J, Stombaugh J, Bittinger K, Bushman FD, Costello EK, et al. QIIME allows analysis of high-throughput community sequencing data. Nature methods. 2010; 7(5):335–6. Epub 2010/04/13. https://doi.org/10.1038/nmeth.f.303 PMID: 20383131.

67. Bragg L, Stone G, Imelfort M, Hugenholtz P, Tyson GW. Fast, accurate error-correction of amplicon pyrosequences using Acacia. Nature methods. 2012; 9(5):425–6. Epub 2012/05/01. https://doi.org/10.1038/nmeth.1990 PMID: 22543370.

68. Edgar RC. UPARSE: highly accurate OTU sequences from microbial amplicon reads. Nature methods. 2013; 10(10):996–8. Epub 2013/08/21. https://doi.org/10.1038/nmeth.2604 PMID: 23955772.

69. Quast C, Pruesse E, Yilmaz P, Gerken J, Schweer T, Yarza P, et al. The SILVA ribosomal RNA gene database project: improved data processing and web-based tools. Nucleic Acids Res. 2013; 41(Database issue):D590–6. Epub 2012/11/30. https://doi.org/10.1093/nar/gks1219 PMID: 23193283.

70. McMurdie PJ, Holmes S. phyloseq: an R package for reproducible interactive analysis and graphics of microbiome census data. PLoS ONE. 2013; 8(4):e61217. Epub 2013/05/01. https://doi.org/10.1371/journal.pone.0061217 PMID: 23630581.

71. Robinson MD, McCarthy DJ, Smyth GK. edgeR: a Bioconductor package for differential expression analysis of digital gene expression data. Bioinformatics. 2010; 26(1):139–40. Epub 2009/11/17. https://doi.org/10.1093/bioinformatics/btp616 PMID: 19910308.

72. Clarke KR, Gorley RN. PRIMER v&: Users Mannual/Tutorial. Plymouth, UK: PRIMER-E; 2015.

73. Meyer F, Paarmann D, D'Souza M, Olson R, Glass EM, Kubal M, et al. The metagenomics RAST server—a public resource for the automatic phylogenetic and functional analysis of metagenomes. BMC Bioinformatics. 2008; 9:386. Epub 2008/09/23. https://doi.org/10.1186/1471-2105-9-386 PMID: 18803844.

74. Kwon MJ, Yang J-S, Shim MJ, Boyanov MI, Kemner KM, O'Loughlin EJ. Acid extraction overestimates the total Fe(II) in the presence of iron (hydr)oxide and sulfide minerals. Environmental Science & Technology Letters. 2014; 1(7):310–4. https://doi.org/10.1021/ez500152h

75. Ramette A. Multivariate analyses in microbial ecology. FEMS Microbiol Ecol. 2007; 62(2):142–60. Epub 2007/09/26. https://doi.org/10.1111/j.1574-6941.2007.00375.x PMID: 17892477.

76. Finneran KT, Johnsen CV, Lovley DR. *Rhodoferax ferrireducens* sp. nov., a psychrotolerant, facultatively anaerobic bacterium that oxidizes acetate with the reduction of Fe(III). Int J Syst Evolut Microbiol. 2003; 53:669–73. https://doi.org/10.1099/ijs.0.02298-0 PMID: 12807184

77. Robertson WJ, Franzmann PD, Mee BJ. Spore-forming, *Desulfosporosinus*-like sulphate-reducing bacteria from a shallow aquifer contaminated with gasoline. Journal of Applied Microbiology. 2000; 88(2):248–59. Epub 2000/03/29. https://doi.org/10.1046/j.1365-2672.2000.00957.x PMID: 10735993.

78. Nevin KP, Finneran KT, Lovley DR. Microorganisms associated with uranium bioremediation in a high-salinity subsurface sediment. Appl Environ Microbiol. 2003; 69(6):3672–5. Epub 2003/06/06. https://doi.org/10.1128/aem.69.6.3672-3675.2003 PMID: 12788780.

79. Church CD, Wilkin RT, Alpers CN, Rye RO, McCleskey RB. Microbial sulfate reduction and metal attenuation in pH 4 acid mine water. Geochemical Transactions. 2007; 8(10). https://doi.org/10.1186/1467-4866-8-10 PMID: 17956615

80. Cardenas E, Wu W-M, Leigh MB, Carley J, Carroll S, Gentry T, et al. Microbial communities in contaminated sediments, associated with bioremediation of uranium to submicromolar levels. Appl Environ Microbiol. 2008; 74(12):3718–29. Epub 2008/05/06. https://doi.org/10.1128/AEM.02308-07 PMID: 18456853.

81. Burkhardt E-M, Akob DM, Bischoff S, Sitte J, Kostka JE, Banerjee D, et al. Impact of biostimulated redox processes on metal dynamics in an iron-rich creek soil in a former uranium mining area. Environ Sci Technol. 2010; 44(1):177–83. Epub 2009/11/27. https://doi.org/10.1021/es902038e PMID: 19938814.

82. Sato Y, Hamai T, Hori T, Aoyagi T, Inaba T, Kobayashi M, et al. *Desulfosporosinus* spp. were the most predominant sulfate-reducing bacteria in pilot- and laboratory-scale passive bioreactors for acid mine drainage treatment. Appl Microbiol Biotechnol. 2019; 103(18):7783–93. Epub 2019/08/08. https://doi.org/10.1007/s00253-019-10063-2 PMID: 31388728.

83. Kaksonen AH, Spring S, Schumann P, Kroppenstedt RM, Puhakka JA. *Desulfovirgula thermocuniculi* gen. nov., sp. nov., a thermophilic sulfate-reducer isolated from a geothermal underground mine in Japan. Int J Syst Evol Microbiol. 2007; 57(Pt 1):98–102. Epub 2007/01/16. https://doi.org/10.1099/ijs.0.64655-0 PMID: 17220449.

84. Lee YJ, Dashti M, Prange A, Rainey FA, Rohde M, Whitman WB, et al. *Thermoanaerobacter sulfurigignens* sp. nov., an anaerobic thermophilic bacterium that reduces 1 M thiosulfate to elemental sulfur and tolerates 90 mM sulfite. Int J Syst Evol Microbiol. 2007; 57(Pt 7):1429–34. Epub 2007/07/13. https://doi.org/10.1099/ijs.0.64748-0 PMID: 17625170.

85. Frolov EN, Zayulina KS, Kopitsyn DS, Kublanov IV, Bonch-Osmolovskaya EA, Chernyh NA. *Desulfothermobacter acidiphilus* gen. nov., sp. nov., a thermoacidophilic sulfate-reducing bacterium isolated from a terrestrial hot spring. Int J Syst Evol Microbiol. 2018; 68(3):871–5. Epub 2018/02/21. https://doi.org/10.1099/ijsem.0.002599 PMID: 29458537.

86. Flynn TM, Sanford RA, Ryu H, Bethke CM, Levine AD, Ashbolt NJ, et al. Functional microbial diversity explains groundwater chemistry in a pristine aquifer. BMC Microbiol. 2013; 13(1):146. Epub 2013/06/27. https://doi.org/10.1186/1471-2180-13-146 PMID: 23800252.

87. Flynn TM, Sanford RA, Santo Domingo JW, Ashbolt NJ, Levine AD, Bethke CM. The active bacterial community in a pristine confined aquifer. Water Resources Research. 2012; 48(9). https://doi.org/10.1029/2011WR011568

88. Nealson KH. Sediment bacteria: who's there, what are they doing, and what's new? Annu Rev Earth Planet Sci. 1997; 25:403–34. Epub 1997/01/01. https://doi.org/10.1146/annurev.earth.25.1.403 PMID: 11540735.

89. Wrighton KC, Castelle CJ, Wilkins MJ, Hug LA, Sharon I, Thomas BC, et al. Metabolic interdependencies between phylogenetically novel fermenters and respiratory organisms in an unconfined aquifer. ISME J. 2014; 8(7):1452–63. Epub 2014/03/14. https://doi.org/10.1038/ismej.2013.249 PMID: 24621521.

90. Hansel CM, Fendorf S, Jardine PM, Francis CA. Changes in bacterial and archaeal community structure and functional diversity along a geochemically variable soil profile. Appl Environ Microbiol. 2008; 74(5):1620–33. Epub 2008/01/15. https://doi.org/10.1128/AEM.01787-07 PMID: 18192411.

91. Haaijer SC, Crienen G, Jetten MS, Op den Camp HJ. Anoxic iron cycling bacteria from an iron sulfide- and nitrate-rich freshwater environment. Frontiers in microbiology. 2012; 3:26. Epub 2012/02/22. https://doi.org/10.3389/fmicb.2012.00026 PMID: 22347219.

92. Snoeyenbos-West OL, Nevin KP, Anderson RT, Lovley DR. Enrichment of Geobacter species in response to stimulation of Fe(III) reduction in sandy aquifer sediments. Microbial Ecology. 2000; 39(2):153–67. Epub 2000/06/01. https://doi.org/10.1007/s002480000018 PMID: 10833228.

93. Coates JD, Phillips EJP, Lonergan DJ, Jenter H, Lovley DR. Isolation of *Geobacter* species from diverse sedimentary environments. Appl Environ Microbiol. 1996; 62(5):1531–6. https://doi.org/10.1128/AEM.62.5.1531-1536.1996 PMID: 8633852

94. Holmes DE, Finneran KT, O'Neil RA, Lovley DR. Enrichment of members of the family *Geobacteraceae* associated with stimulation of dissimilatory metal reduction in uranium-contaminated aquifer sediments. Appl Environ Microbiol. 2002; 68(5):2300–6. https://doi.org/10.1128/aem.68.5.2300-2306.2002 PMID: 11976101

95. Elifantz H, N'Guessan LA, Mouser PJ, Williams KH, Wilkins MJ, Risso C, et al. Expression of acetate permease-like (apl) genes in subsurface communities of Geobacter species under fluctuating acetate concentrations. FEMS Microbiol Ecol. 2010; 73(3):441–9. Epub 2010/06/11. https://doi.org/10.1111/j.1574-6941.2010.00907.x PMID: 20533942.

96. North NN, Dollhopf ME, Petrie L, Istok JD, Balkwill DL, Kostka JE. Change in bacterial community structure during in situ biostimulation of subsurface sediment contaminated with uranium and nitrate. Appl Environ Microbiol. 2004; 70(8):4911–20. https://doi.org/10.1128/AEM.70.8.4911-4920.2004 PMID: 15294831

97. N'Guessan AL, Vrionis HA, Resch CT, Long PE, Lovley DR. Sustained removal of uranium from contaminated groundwater following stimulation of dissimilatory metal reduction. Environ Sci Technol. 2008; 42(8):2999–3004. https://doi.org/10.1021/es071960p PMID: 18497157

98. Hori T, Muller A, Igarashi Y, Conrad R, Friedrich MW. Identification of iron-reducing microorganisms in anoxic rice paddy soil by ^{13}C-acetate probing. ISME J. 2010; 4(2):267–78. Epub 2009/09/25. https://doi.org/10.1038/ismej.2009.100 PMID: 19776769.

99. Marquart KA, Haller BR, Paper JM, Flynn TM, Boyanov MI, Shodunke G, et al. Influence of pH on the balance between methanogenesis and iron reduction. Geobiology. 2019; 17(2):185–98. Epub 2018/11/06. https://doi.org/10.1111/gbi.12320 PMID: 30387274.

100. Rowland HAL, Pederick RL, Polya DA, Pancost RD, Van Dongen BE, Gault AG, et al. The control of organic matter on microbially mediated iron reduction and arsenic release in shallow alluvial aquifers, Cambodia. Geobiology. 2007; 5(3):281–92. https://doi.org/10.1111/j.1472-4669.2007.00100.x

101. Kirk MF, Santillan EFU, Sanford RA, Altman SJ. CO2-induced shift in microbial activity affects carbon trapping and water quality in anoxic bioreactors. Geochimica et Cosmochimica Acta. 2013; 122:198–208. https://doi.org/10.1016/j.gca.2013.08.018

102. Xu J, Zhuang L, Yang G, Yuan Y, Zhou S. Extracellular quinones affecting methane production and methanogenic community in paddy soil. Microb Ecol. 2013; 66(4):950–60. Epub 2013/08/06. https://doi.org/10.1007/s00248-013-0271-7 PMID: 23913198.

103. Chen M, Tong H, Liu C, Chen D, Li F, Qiao J. A humic substance analogue AQDS stimulates *Geobacter* sp. abundance and enhances pentachlorophenol transformation in a paddy soil. Chemosphere. 2016; 160:141–8. Epub 2016/07/04. https://doi.org/10.1016/j.chemosphere.2016.06.061 PMID: 27372263.

104. Komlos J, Jaffé PR. Effect of iron bioavailability on dissolved hydrogen concentrations during microbial iron reduction. Biodegrad. 2004; 15:315–25. https://doi.org/10.1023/b:biod.0000042187.31072.60 PMID: 15523914

105. Kwon MJ, O'Loughlin EJ, Boyanov MI, Brulc JM, Johnston ER, Kemner KM, et al. Impact of organic carbon electron donors on microbial community development under iron- and sulfate-reducing conditions. PLoS ONE. 2016:1–22. https://doi.org/10.1371/journal.pone.0146689 PMID: 26800443

106. Handley KM, Wrighton KC, Miller CS, Wilkins MJ, Kantor RS, Thomas BC, et al. Disturbed subsurface microbial communities follow equivalent trajectories despite different structural starting points. Environ Microbiol. 2014; 17(3):622–36. Epub 2014/03/29. https://doi.org/10.1111/1462-2920.12467 PMID: 24674078.

107. Geets J, Borremans B, Vangronsveld J, Diels L, van der Lelie D. Molecular monitoring of SBR community structure and dynamics in batch experiments to examine the applicability of *in situ* precipitation of heavy metals for groundwater remediation. Journal of Soils and Sediments. 2005; 5(3):149–63. https://doi.org/10.1065/jss2004.12.125

108. Stackebrandt E, Sproer C, Rainy FA, Burghardt J, Päuker O, Hippe H. Phylogenetic analysis of the genus *Desulfotomaculum*: Evidence for the misclassification of *Desulfotomaculum guttoideum* and description of *Desulfotomaculum orientis* as *Desulfosporosinus orientis* gen. nov., comb. nov. Int J Syst Bacteriol. 1997; 47(4):1134–9. https://doi.org/10.1099/00207713-47-4-1134 PMID: 9336920

109. Robertson WJ, Bowman JP, Franzmann PD, Mee BJ. *Desulfosporosinus meridiei* sp. nov., a spore-forming sulfate-reducing bacterium isolated from gasoline-contaminated groundwater. Int J Syst Evolut Microbiol. 2001; 51:133–40.

110. Stackebrandt E, Schumann P, Schüler E, Hippe H. Reclassification of *Desulfotomaculum auripigmentum* as *Desulfosporosinus auripigmenti* corrig., comb. nov. Int J Syst Evolut Microbiol. 2003; 53:1439–43. https://doi.org/10.1099/ijs.0.02526-0 PMID: 13130030

111. Ramamoorthy S, Sass H, Langner H, Schumann P, Kroppenstedt RM, Spring S, et al. *Desulfosporosinus lacus* sp. nov., a sulfate-reducing bacterium isolated from pristine freshwater lake sediments. Int J Syst Evolut Microbiol. 2006; 56(Pt 12):2729–36. Epub 2006/12/13. https://doi.org/10.1099/ijs.0.63610-0 PMID: 17158969.

112. Vatsurina A, Badrutdinova D, Schumann P, Spring S, Vainshtein M. *Desulfosporosinus hippei* sp. nov., a mesophilic sulfate-reducing bacterium isolated from permafrost. Int J Syst Evolut Microbiol. 2008; 58:1228–32. https://doi.org/10.1099/ijs.0.65368-0 PMID: 18450718

113. Lee Y-J, Romanek CS, Wiegel J. *Desulfosporosinus youngiae* sp. nov., a spore-forming, sulfate-reducing bacterium isolated from a constructed wetland treating acid mine drainage. Int J Syst Evolut Microbiol. 2009; 59:2743–6. https://doi.org/10.1099/ijs.0.007336-0 PMID: 19625426

114. Alazard D, Joseph M, Battaglia-Brunet F, Cayol JL, Ollivier B. *Desulfosporosinus acidiphilus* sp. nov.: a moderately acidophilic sulfate-reducing bacterium isolated from acid mining drainage sediments: New taxa: Firmicutes (Class Clostridia, Order Clostridiales, Family Peptococcaceae). Extremophiles. 2010; 14(3):305–12. Epub 2010/04/02. https://doi.org/10.1007/s00792-010-0309-4 PMID: 20358236.

115. Mayeux B, Fardeau ML, Bartoli-Joseph M, Casalot L, Vinsot A, Labat M. *Desulfosporosinus burensis* sp. nov., a spore-forming, mesophilic, sulfate-reducing bacterium isolated from a deep clay environment. Int J Syst Evol Microbiol. 2013; 63(Pt 2):593–8. Epub 2012/05/01. https://doi.org/10.1099/ijs.0.035238-0 PMID: 22544786.

116. Sanchez-Andrea I, Stams AJ, Hedrich S, Nancucheo I, Johnson DB. *Desulfosporosinus acididurans* sp. nov.: an acidophilic sulfate-reducing bacterium isolated from acidic sediments. Extremophiles. 2015; 19(1):39–47. Epub 2014/11/06. https://doi.org/10.1007/s00792-014-0701-6 PMID: 25370366.

117. Mardanov AV, Panova IA, Beletsky AV, Avakyan MR, Kadnikov VV, Antsiferov DV, et al. Genomic insights into a new acidophilic, copper-resistant *Desulfosporosinus* isolate from the oxidized tailings area of an abandoned gold mine. FEMS Microbiol Ecol. 2016; 92(8). Epub 2016/05/26. https://doi.org/10.1093/femsec/fiw111 PMID: 27222219.

118. Vandieken V, Niemann H, Engelen B, Cypionka H. *Marinisporobacter balticus* gen. nov., sp. nov., *Desulfosporosinus nitroreducens* sp. nov. and *Desulfosporosinus fructosivorans* sp. nov., new spore-forming bacteria isolated from subsurface sediments of the Baltic Sea. Int J Syst Evol Microbiol. 2017; 67(6):1887–93. Epub 2017/06/25. https://doi.org/10.1099/ijsem.0.001883 PMID: 28646634.

119. Cord-Ruwisch R, Lovley D, Schink B. Growth of *Geobacter sulfurreducens* with acetate in syntrophic cooperation with hydrogen-oxidizing anaerobic partners. Appl Environ Microbiol. 1998; 64(6):2232–6. https://doi.org/10.1128/AEM.64.6.2232-2236.1998 PMID: 9603840

120. Kimura Z, Okabe S. Acetate oxidation by syntrophic association between *Geobacter sulfurreducens* and a hydrogen-utilizing exoelectrogen. ISME J. 2013; 7(8):1472–82. Epub 2013/03/15. https://doi.org/10.1038/ismej.2013.40 PMID: 23486252.

121. Klemps R, Cypionka H, Widdel F, Pfennig N. Growth with hydrogen, and further physiological characteristics of *Desulfotomaculum* species. Archives of Microbiology. 1985; 143(2):203–8.

122. Kwon MJ, Boyanov MI, Antonopoulos DA, Brulc JM, Johnston ER, Skinner KA, et al. Effects of dissimilatory sulfate reduction on FeIII (hydr)oxide reduction and microbial community development. Geochim Cosmochim Acta. 2014; 129(12):4570–6. https://doi.org/10.1016/j.gca.2013.09.037

123. Hansel CM, Lentini CJ, Tang Y, Johnston DT, Wankel SD, Jardine PM. Dominance of sulfur-fueled iron oxide reduction in low-sulfate freshwater sediments. ISME J. 2015; 9(11):2400–12. Epub 2015/04/15. https://doi.org/10.1038/ismej.2015.50 PMID: 25871933.

124. Berg JS, Jezequel D, Duverger A, Lamy D, Laberty-Robert C, Miot J. Microbial diversity involved in iron and cryptic sulfur cycling in the ferruginous, low-sulfate waters of Lake Pavin. PLoS ONE. 2019; 14(2):e0212787. Epub 2019/02/23. https://doi.org/10.1371/journal.pone.0212787 PMID: 30794698.

125. Wu S, Zhao Y, Chen Y, Dong X, Wang M, Wang G. Sulfur cycling in freshwater sediments: A cryptic driving force of iron deposition and phosphorus mobilization. Sci Total Environ. 2019; 657:1294–303. Epub 2019/01/27. https://doi.org/10.1016/j.scitotenv.2018.12.161 PMID: 30677896.

126. Chapelle FH, Lovley DR. Competetive exclusion of sulfate reduction by Fe(III)-reducing bacteria: A mechanism for producing discrete zones of high-iron ground water. Ground Water. 1992; 30(1):29–36.

127. Jakobsen R, Postma D. Redox zoning, rates of sulfate reduction and interactions with Fe-reduction and methanogenesis in a shallow sandy aquifer, Rømø, Denmark. Geochim Cosmochim Acta. 1999; 63(1):137–51.

128. Yu RQ, Flanders JR, Mack EE, Turner R, Mirza MB, Barkay T. Contribution of coexisting sulfate and iron reducing bacteria to methylmercury production in freshwater river sediments. Environ Sci Technol. 2012; 46(5):2684–91. Epub 2011/12/14. https://doi.org/10.1021/es2033718 PMID: 22148328.

129. Akob DM, Mills HJ, Gihring TM, Kerkhof L, Stucki JW, Anastacio AS, et al. Functional diversity and electron donor dependence of microbial populations capable of U(VI) reduction in radionuclide-contaminated subsurface sediments. Appl Environ Microbiol. 2008; 74(10):3159–70. Epub 2008/04/02. https://doi.org/10.1128/AEM.02881-07 PMID: 18378664.

130. Bethke CM, Ding D, Jin Q, Sanford RA. Origin of microbiological zoning in groundwater flows. Geology. 2008; 36(9):739–42. https://doi.org/10.1130/G24859a.1

131. Bethke CM, Sanford RA, Kirk MF, Jin Q, Flynn TM. The thermodynamic ladder in geomicrobiology. American Journal of Science. 2011; 311(3):183–210. https://doi.org/10.2475/03.2011.01